

Two-particle Bose-Einstein correlations and their Lévy parameters in PbPb collisions at $\sqrt{s_{NN}} = 5.02$ TeV

A. Tumasyan *et al.**
(CMS Collaboration)



(Received 20 June 2023; accepted 9 November 2023; published 23 February 2024)

Two-particle Bose–Einstein momentum correlation functions are studied for charged-hadron pairs in lead-lead collisions at a center-of-mass energy per nucleon pair of $\sqrt{s_{NN}} = 5.02$ TeV. The data sample, containing 4.27×10^9 minimum bias events corresponding to an integrated luminosity of 0.607 nb^{-1} , was collected by the CMS experiment in 2018. The experimental results are discussed in terms of a Lévy-type source distribution. The parameters of this distribution are extracted as functions of particle pair average transverse mass and collision centrality. These parameters include the Lévy index or shape parameter α , the Lévy scale parameter R , and the correlation strength parameter λ . The source shape, characterized by α , is found to be neither Cauchy nor Gaussian, implying the need for a full Lévy analysis. Similarly to what was previously found for systems characterized by Gaussian source radii, a hydrodynamical scaling is observed for the Lévy R parameter. The λ parameter is studied in terms of the core-halo model.

DOI: [10.1103/PhysRevC.109.024914](https://doi.org/10.1103/PhysRevC.109.024914)

I. INTRODUCTION

The effect of quantum statistics is evident in the momentum correlations observed for identical particles emitted in high-energy hadronic and nuclear collisions. These correlations were first studied using pion pairs produced in proton-antiproton collisions [1], where they were explained by the Bose–Einstein nature of pions [2]. Subsequent to the first Bose–Einstein momentum correlation measurements, it was shown [3–5] that the particle correlations are closely related to earlier intensity correlation measurements used to determine the angular diameters of stars, as performed by Hanbury Brown and Twiss [6], and are now referred to as HBT correlations. The observed momentum correlations can be related to the spatiotemporal particle emission probability, the so-called “source distribution,” through a Fourier transform. This allows for a determination of the spatial structure of the particle-emitting source at the femtometer scale.

Measuring and interpreting such momentum correlations is called “femtoscopy” and these studies have significantly advanced our understanding of the processes governing heavy ion collisions [7]. The fluid nature of the strongly coupled quark-gluon plasma created in heavy ion collisions was established, in part, by Bose–Einstein correlation measurements [8]. In particular, the pair transverse momentum dependence of the Gaussian source radii [8–10] can be explained as a consequence of the hydrodynamical expansion of the medium

[11,12]. In addition, the measured source radii provide information on the transition from a quark-gluon plasma to a hadronic state of matter [13,14] and have also been important for extending our understanding of quantum chromodynamics to new regions of phase space [15].

In past femtoscopic measurements, either Gaussian [8,16–18] or Cauchy [19,20] source distributions have generally been assumed. However, recent high-precision correlation measurements in gold-gold (AuAu) collisions at a center-of-mass energy per nucleon pair of $\sqrt{s_{NN}} = 200$ GeV at the BNL Relativistic Heavy Ion Collider (RHIC) [21] and in beryllium-beryllium collisions at 150A GeV/c beam momentum at the CERN Super Proton Synchrotron (SPS) [22] have shown that neither the Gaussian nor the Cauchy approximation can adequately reproduce the measured results. Rather, a generalization of these distributions, the so-called Lévy alpha-stable distribution [23], is required to describe the data. The Lévy exponent α quantifies the deviation of the source shape from a Gaussian distribution and may be influenced by various physical processes [24–28].

In this paper, the source geometry is investigated for lead-lead (PbPb) collisions at $\sqrt{s_{NN}} = 5.02$ TeV by measuring quantum-statistical two-particle Bose–Einstein correlations of unidentified charged hadrons. The measured correlation functions are fitted with a formula based on a Lévy source distribution, allowing for the possibility of a non-Gaussian source shape. The extracted source parameters are studied as functions of pair transverse momentum and collision geometry.

The paper is structured as follows: The theory of Bose–Einstein correlations and the connection between the two-particle correlation function and the geometry of the particle emitting source are discussed in Sec. II. The experimental setup is described in Sec. III. The analysis details and systematic uncertainties are discussed in Sec. IV. The results are

*Full author list given at the end of the article.

presented and discussed in Sec. V, with a summary presented in Sec. VI. Tabulated results are provided in the HEPData record for this analysis [29].

II. BOSE-EINSTEIN CORRELATIONS

The general definition of the two-particle momentum correlation function is given by

$$C_2(p_1, p_2) = \frac{N_{12}(p_1, p_2)}{N_1(p_1)N_2(p_2)}, \quad (1)$$

where p_1 and p_2 are the particle four-momenta, $N_1(p_1)$ and $N_2(p_2)$ are the single-particle momentum distributions, and $N_{12}(p_1, p_2)$ is the two-particle momentum distribution. For identical bosons in high-multiplicity heavy ion collisions, the main source of correlations is the Bose-Einstein effect [21]. This can be understood if one expresses the momentum distributions in terms of the source distribution, $S(x, p)$, which is defined as the probability density distribution of creating a particle with four-momentum p at space-time point x . As shown in Refs. [30,31], in the approximation that $p_1 \approx p_2 \approx K$, with $K = (p_1 + p_2)/2$ being the average four-momentum, the relationship between the correlation function and the source distribution becomes

$$C_2^{(0)}(Q, K) = 1 + \frac{|\tilde{S}(Q, K)|^2}{|\tilde{S}(0, K)|^2}, \quad (2)$$

where $\tilde{S}(Q, K)$ is the Fourier transform of the source distribution,

$$\tilde{S}(Q, K) = \int S(x, K) e^{iQx} d^4x, \quad (3)$$

with $Q = p_1 - p_2$ denoting the relative four-momentum of the two particles. In Eq. (2), the superscript (0) denotes that final-state interactions of hadrons, such as the Coulomb interaction, are ignored. The effect of the Coulomb interaction will be discussed later in this section.

The above expressions imply $C_2^{(0)}(Q = 0, K) = 2$. This cannot be directly verified since the two-particle resolution limits the measurement of C_2 at small values of relative momentum Q . However, based on extrapolations of observed correlation functions, it is found that, in general, $C_2^{(0)}(Q \rightarrow 0) < 2$. This observation has led to the development of a “core-halo” picture [32–36], where the particle-emitting source is divided into two parts: a core of primordial hadrons (including also the decay products of short lived resonances) and a halo of long-lived resonances. The latter is experimentally unresolvable due to its large size that corresponds to very small momentum difference in Fourier space. Taking S to represent the core part of the source and λ as the square of the core fraction, one obtains

$$C_2^{(0)}(Q, K) = 1 + \lambda \frac{|\tilde{S}(Q, K)|^2}{|\tilde{S}(0, K)|^2}, \quad (4)$$

with

$$\lambda = \left(\frac{N_{\text{core}}}{N_{\text{core}} + N_{\text{halo}}} \right)^2. \quad (5)$$

Here N_{core} is the number of hadrons in the core (for a given species) and N_{halo} is the number of hadrons in the halo. The λ parameter is called the correlation strength, because it qualitatively describes how strong the two-particle correlation is. Other approaches to account for the effect of resonances are discussed in Refs. [34–36].

Using Eq. (4), the correlation function can be calculated for an assumed source distribution, with the parameters of the source distribution then determined by fits to the experimental results. The Gaussian, Cauchy, and a generalization of these two distribution functions, the so-called Lévy alpha-stable distribution, have been studied in Ref. [21]. The motivation behind these studies is that the mean-free path increases over time in an expanding hadron gas. Hence, if one describes the evolution of hadrons by generating random steps, the distribution of the size of these steps may not have a finite variance. In this case, the central limit theorem cannot be applied, thus the limiting distribution of the sum of step sizes for a given hadron is not a Gaussian. This effect has been referred to as “anomalous diffusion.” However, a more generalized version of the central limit theorem is applicable and the limiting distribution in this case falls in the class of symmetric Lévy alpha-stable distributions [37,38], defined as

$$\mathcal{L}(\mathbf{r}; \alpha, R) = \frac{1}{(2\pi)^3} \int d^3q e^{i\mathbf{q}\cdot\mathbf{r}} e^{-\frac{1}{2}|\mathbf{q}R|^\alpha}, \quad (6)$$

with \mathbf{r} being the variable of the distribution and \mathbf{q} being an arbitrary integration variable. In this paper, $\mathcal{L}(\mathbf{r}; \alpha, R)$ is assumed for the shape of the source distribution, i.e., S mentioned above [and used in Eq. (3)] is assumed to be a Lévy distribution \mathcal{L} , with parameters α and R depending on average momentum K . In this case, R is the Lévy scale parameter and α is the Lévy index of stability. Stability means that for $\alpha \leq 2$ this distribution represents the limit of properly normalized sums of independent random variables, and the sum of Lévy distributed random variables (with the same stability index) is also Lévy distributed. The Gaussian distribution is obtained with $\alpha = 2$ and the Cauchy distribution is obtained with $\alpha = 1$. A value of $\alpha > 2$ is not physically allowed for a stable Lévy distribution (as discussed in Ref. [23]). The α parameter describes the shape of the source and its deviation from the Gaussian distribution. In case of a Gaussian source, R is simply the quadratic mean of the distribution. However, for $\alpha < 2$, the stable distributions do not have a second moment. In those cases, R is still proportional to the full width at half maximum (with the proportionality constant depending on α), and therefore represents the spatial scale of the source. The above considerations lead to the following correlation function for a general value of α [38]:

$$C_2^{(0)}(q) = 1 + \lambda e^{-(qR)^\alpha}. \quad (7)$$

Here q is a one-dimensional (1-D) variable, the magnitude of the spatial part of Q in a given frame: $q = |Q|$. The dependence on the average momentum K is carried by the parameters λ , α , and R [21].

The above formulas are based on a planewave analysis and are only valid for interaction-free particles. Final-state interactions distort this simple picture. In the so-called

Bowler–Sinyukov method [39], the most significant final-state interaction in case of charged particles, the Coulomb interaction, is handled by including a correction term $K_C(q; R, \alpha)$, with

$$C_2(q) = 1 - \lambda + \lambda(1 + e^{-(qR)^\alpha})K_C(q; R, \alpha). \quad (8)$$

This correction can be calculated based on the Coulomb wave function, as determined by solving the two-particle Schrödinger equation [21,40]. Such a calculation requires numerical integration of the Lévy distribution multiplied by the square of the absolute value of the Coulomb wave function. A parametrization of the results of this calculation, as a function of R and α , is given in Ref. [40]. The measured correlation functions are fitted with the formula described in Eq. (8).

III. THE CMS DETECTOR

The CMS detector is built around a superconducting solenoid of 6 m internal diameter. Within the solenoid volume are a silicon pixel and strip tracker, a lead tungstate crystal electromagnetic calorimeter ($|\eta| < 3$), and a brass and scintillator hadron calorimeter ($|\eta| < 3$), each composed of a barrel and two endcap sections, where η is the pseudorapidity. In addition to the barrel and endcap detectors, quartz-fiber Cherenkov hadron forward (HF) calorimeters ($3 < |\eta| < 5$) complement the coverage provided by the barrel and endcap detectors on either side of the interaction point. These HF calorimeters are - in ϕ into 20° modular wedges and further segmented to form $0.175 \times 0.175 (\Delta\eta \times \Delta\phi)$ “towers,” where ϕ is the azimuthal angle. A muon system located outside the solenoid and embedded in the steel flux-return yoke is used for the reconstruction and identification of muons with $|\eta| < 2.4$.

The silicon tracker measures the properties of charged particles with $|\eta| < 2.5$. During the 2018 LHC running period corresponding to the data used in this paper, the silicon tracker consisted of 1856 silicon pixels and 15 148 silicon strip detector modules. Details on the pixel detector can be found in Ref. [41]. For nonisolated particles with a transverse momentum of $1 < p_T < 10 \text{ GeV}/c$ and $|\eta| < 2.5$, the track resolutions are typically 1.5% in p_T and $20 - 75 \mu\text{m}$ in the transverse impact parameter (d_{xy}) [42]. Events of interest are selected using a two-tiered trigger system [43]. The first level, composed of custom hardware processors, uses information from the calorimeters and muon detectors to select events at a rate of around 100 kHz. The second level, known as the high-level trigger, consists of a farm of processors running a version of the full event reconstruction software optimized for fast processing and reduces the event rate to around 1 kHz before data storage. A detailed description of the CMS detector, together with a definition of the coordinate system and kinematic variables, can be found in Ref. [44].

IV. MEASUREMENT DETAILS

A. Event and track selection

The analysis presented in this paper used 4.27×10^9 minimum bias triggered events, corresponding to an integrated

luminosity of 0.607 nb^{-1} [45,46], from PbPb collisions collected by the CMS experiment during the 2018 LHC run at $\sqrt{s_{\text{NN}}} = 5.02 \text{ TeV}$. The minimum bias events were triggered by requiring signals above thresholds in the range of $\approx 6 - 12 \text{ GeV}$ energy in at least one channel of each of the HF calorimeters [43]. Further selections were applied to reject events from beam-gas interactions and nonhadronic collisions [47]. Events were also required to have precisely one interaction vertex, reconstructed based on two or more tracks, and within a distance of less than 15 cm from the center of the nominal interaction point along the beam axis. The shapes of the clusters in the pixel detector had to be compatible with those expected from particles produced at the interaction vertex location. After these selections, 2.65×10^9 usable events were obtained. The event centrality was calculated from the transverse energy deposited in both HF calorimeters, using the methodology detailed in Ref. [48]. The centrality describes the fraction of the total inelastic hadronic cross section and is connected to the degree of overlap of the two incident nuclei, with 0% corresponding to the most central (total overlap) and 100% to the least central (least overlap) collisions.

Only the standard CMS *highPurity* tracks defined in Ref. [49] were used for the analysis. Furthermore, individual particles were required to have $p_T > 0.5 \text{ GeV}/c$ with a relative uncertainty $\delta p_T < 10\%$. To focus on midrapidity Bose–Einstein correlations, the analysis was restricted to tracks with $|\eta| < 0.95$. As the correlation function parameters depend on the average pseudorapidity of the considered pair [50], this limited pseudorapidity interval provides a cleaner data sample where the correlation function shape is not influenced by the η dependence. Tracks were required to have at least two hits ($N_{\text{pixel-hit}}$) in the silicon pixel detector, to have at least 11 hits (N_{hit}) in the strip tracking detector, and to have a relative χ^2 of the track fit [$\chi^2 / (N_{\text{dof}} N_{\text{layer}})$] of less than 0.18, where N_{dof} is the number of degrees of freedom during the track fitting and N_{layer} is the number of tracking layers used out of the ten barrel and four pixel layers. A reconstructed track is only considered as a candidate track from the vertex if the significance of the separation along the beam axis z between the track and the best vertex, $|d_z/\sigma(d_z)|$, and the significance of the track impact parameter measured in a plane transverse to the beam, $|d_{xy}/\sigma(d_{xy})|$, are each less than three.

In CMS, particle identification in central to midcentral PbPb collisions is hindered by the overlapping strip tracker clusters in a high track density environment. Therefore, in this measurement, no particle identification was done, and all charged-particle tracks were used. The approach presented in Sec. II is only applicable for a single-particle species, hence it was assumed that all detected charged particles are pions. Depending on the transverse mass and the centrality range, 60%–90% of the investigated particles are pions [51]. It was found that this assumption does not modify the physical results, apart from the λ parameter. This is because the HBT peak in the correlation function at low q is not modified by nonidentical particle pairs or by identical particle pairs of species that have been misidentified as pions and, therefore, calculated to have the wrong q value. The effect of the lack of particle identification on the λ parameter is discussed in Sec. V C.

B. Event mixing and pair selection

For determining the correlation functions, two distributions are formed: a signal (actual) distribution $A(q)$ of pairs containing the Bose–Einstein correlation, and a background distribution $B(q)$, using the event mixing method to correct for correlations not stemming from quantum statistics or final-state interactions. The signal pair distribution is formed with pairs of particles belonging to the same event. The q variable is taken as the absolute value of the three-dimensional (3-D) momentum difference ($|q|_{\text{LCMS}}$) in the longitudinally comoving frame (LCMS), which is the reference system where the longitudinal component of the average pair momentum is zero. This distribution is affected by various effects resulting from the event kinematics and the detector acceptance. To correct for these effects a background distribution is created with particle pairs taken from different events. For this purpose, a pool of events is formed based on centrality (within a width of 10%) and collision vertex location (within 3 cm in z vertex). Then, for each data event, a mixed event was formed using the pool associated with the data event class, making sure that each particle of this mixed event belongs to a different data event. Pairs within the mixed events were used to create the above-mentioned $B(q)$ distribution. More details about the event mixing can be found in Refs. [21,52]. The $A(q)$ and $B(q)$ distributions were divided and normalized to obtain the correlation function

$$C_2(q) = \frac{A(q) \int_{q_1}^{q_2} B(q) dq}{B(q) \int_{q_1}^{q_2} A(q) dq}. \quad (9)$$

The integrals are performed over a range $[q_1, q_2] = [4.8, 6.4] \text{ GeV}/c$ where the correlation function is not expected to exhibit quantum-statistical features, which are only present for $q \lesssim 0.2 \text{ GeV}/c$ [21,53], for source sizes of several femtometers.

Tracking efficiency correction factors were used as weights when measuring pair distributions. Each reconstructed track was weighted by the inverse of the efficiency factor, $\epsilon_{\text{trk}}(\eta, p_{\text{T}}, \text{centrality})$. The efficiency weighting factor accounts for the reconstruction efficiency \mathcal{E}_{r} and the fraction of misidentified tracks, with $f_{\text{fake}}(\eta, p_{\text{T}}, \text{centrality})$ and $\epsilon_{\text{trk}} = \mathcal{E}_{\text{r}}/(1 - f_{\text{fake}})$.

The obtained correlation functions exhibit effects stemming from the finite segmentation of the detectors and the imperfect tracking algorithm, allowing for tracks to split into two reconstructed particles, or separate tracks to merge into a single reconstructed particle. To remove these effects from our sample, a two-dimensional (2-D) histogram of pseudorapidity difference $\Delta\eta$ vs azimuthal angle difference $\Delta\phi$ was studied for the track pairs. A uniform distribution outside of a small $\Delta\eta$ and $\Delta\phi$ region was found, with the detector artifacts limited to this small region. The pairs were then required to satisfy the condition

$$\left(\frac{|\Delta\eta|}{\Delta\eta_{\min}} \right)^2 + \left(\frac{|\Delta\phi|}{\Delta\phi_{\min}} \right)^2 > 1, \quad (10)$$

with $\Delta\eta_{\min} = 0.014$ and $\Delta\phi_{\min} = 0.022$, to select pairs free of these artifacts.

While in this analysis the correlation function is determined in terms of $|q|_{\text{LCMS}}$, it can also be expressed in terms of the absolute value of the invariant momentum difference, q_{inv} [21,54], which is the absolute value of the momentum difference in the pair center-of-mass system. Correlation functions depending on the transverse and longitudinal components of the 3-D momentum difference, as well as on the energy difference, were investigated. It was found that the correlation functions had their maximal values for small $|q|_{\text{LCMS}}$, rather than small q_{inv} values, indicating that the most sensitive 1-D variable of the measured correlations is $|q|_{\text{LCMS}}$, hence the choice $q \equiv |q|_{\text{LCMS}}$ to investigate the physics parameters.

In the LCMS, the longitudinal component of the average momentum K vanishes. In this case, the Fourier transform of the source distribution \tilde{S} can be expressed in terms of the transverse component K_{T} of the average momentum. Alternatively, the transverse mass, $m_{\text{T}} = ([b]m^2 + K_{\text{T}}^2)^{1/2}$, may be used, if the mass m of the investigated particle species is known. The current analysis is done in ranges of the K_{T} variable, with the results expressed in terms of m_{T} . Here, the pion mass is assumed, to facilitate comparisons with other experimental results and with theory.

C. Correlation functions

The $A(q)$ and $B(q)$ distributions were measured up to $q = 8 \text{ GeV}/c$ in 24 ranges of K_{T} from 0.5 to $1.9 \text{ GeV}/c$ and in six centrality classes (0%–5%, 5%–10%, 10%–20%, 20%–30%, 30%–40%, 40%–60%). Negative and positive same-charged hadron pairs were measured separately. In each case, the correlation function $C_2(q)$ was calculated. Although no significant difference was observed between the positively and the negatively charged pairs, the two cases were treated separately to identify minor discrepancies. While the Bose–Einstein peak for these correlation functions occurs for $q < 200 \text{ MeV}/c$, a structure was also observed in the $C_2(q)$ distributions at higher q values. This higher q structure can be attributed to a number of possible sources, including energy and momentum conservation, resonance decays, bulk flow phenomena [19], and minijets [19]. We addressed this by fitting the following empirically determined functional form [19,53,55] to the long-range background:

$$BG(q) = N(1 + \alpha_1 e^{-(qR_1)^2})(1 - \alpha_2 e^{-(qR_2)^2}), \quad (11)$$

where N , α_1 , α_2 , R_1 , and R_2 are fit parameters. An example fit to the experimental data using Eq. (11) is shown in Fig. 1. The correlation function $C_2(q)$ was then divided by the long-range background function $BG(q)$, resulting in the double-ratio correlation function

$$DR(q) = \frac{C_2(q)}{BG(q)}. \quad (12)$$

The large- q background is close to constant on the scale of the Bose–Einstein peak, i. e., over a range of few times $10 \text{ MeV}/c$. Consequently, this correction is not as important as was found for proton-proton collisions [53], where the much smaller source radii lead to much wider correlation functions.

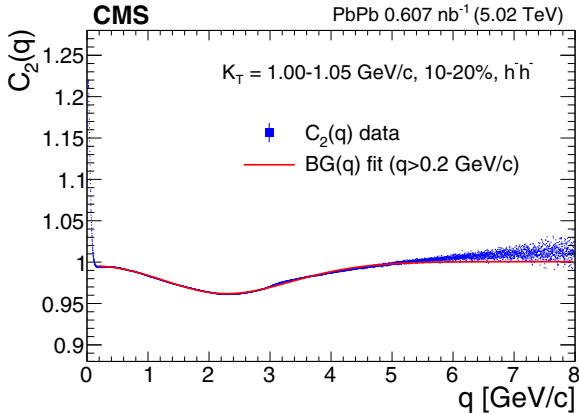


FIG. 1. An example of a long-range background fit to the correlation function $C_2(q)$ of negatively charged hadron pairs with $1.00 < K_T < 1.05 \text{ GeV}/c$ in the 10%–20% centrality bin. The Bose-Einstein peak is below $q = 0.2 \text{ GeV}/c$, therefore the $0.2 < q < 8.0 \text{ GeV}/c$ region was used for the long-range background fit.

D. Lévy fits to correlation functions

The double-ratio correlation function $DR(q)$ removes most effects other than the quantum-statistical correlation and the final-state interactions. This function was fit with an extension of Eq. (8) that allows for a possible residual linear background:

$$DR(q) = N[1 - \lambda + \lambda(1 + e^{-(qR)^\alpha})K_C(q; R, \alpha)](1 + \epsilon q). \quad (13)$$

Here R is the Lévy scale parameter, α is the Lévy stability index, and λ is the correlation strength. The empirical normalization parameter N and linear background parameter ϵ are needed to remove any remaining background effects in the double-ratio correlation function. The Coulomb correction factor $K_C(q; R, \alpha)$ is calculated based on Ref. [40].

The fitting was performed using the MINUIT2 package [56,57] by standard χ^2 minimization. The asymmetric statistical uncertainties were calculated using the MINOS package [56,57]. A fit is deemed statistically acceptable if the confidence level calculated from the χ^2 value and the number of degrees of freedom is above 0.1%. The convergence of each fit together with a positive-definite covariance matrix was also required. Furthermore, the stability of the fit parameters versus the binning of $DR(q)$ was tested, and no modification in the values of the parameters was found. Figure 2 shows the results of a typical fit.

Upper and lower limits in q were set for the fitted region. For large q values, the correlation no longer exhibits any features beyond those resulting from the residual long-range background. For very small q values, the data are strongly affected by the finite momentum resolution and pair reconstruction efficiency of the detectors, as well as the details of the pair selection. These effects were investigated with detailed Monte Carlo simulations based on HYDJET (version 1.8, tune “Drum” [58]) events, where the detector response was simulated using GEANT4 [59], and a considerable decrease of pair reconstruction efficiency was found at low q values,

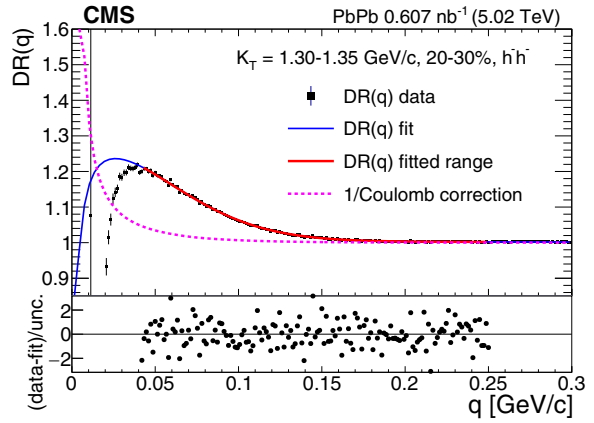


FIG. 2. An example fit to the double-ratio correlation function $DR(q)$ of negatively charged hadron pairs with $1.30 < K_T < 1.35 \text{ GeV}/c$ in the 20%–30% centrality bin. The error bars show the statistical uncertainties. The fitted function is shown in blue, while the red overlay indicates the range used for the fit. The size of the Coulomb correction is indicated in magenta. The lower panel shows the deviation of the fit from the data in each bin in units of the standard deviation in that bin.

below approximately 50 MeV/c, as shown in Fig. 3. Moreover, it has previously been shown in Refs. [40,60] that the sharp decrease of the correlation function for very low q values does not depend on the exact source shape, but is rather determined by the Gamow factor that corresponds to the spatial integral of the relative wave function squared multiplied by a point-like source [53]. This very-low- q behavior of the fit function is found to be unaffected when calculated with various source and final-state interaction assumptions [60]. For the present analysis, the lower and upper fit limits were selected independently for each centrality and K_T class, with the lower

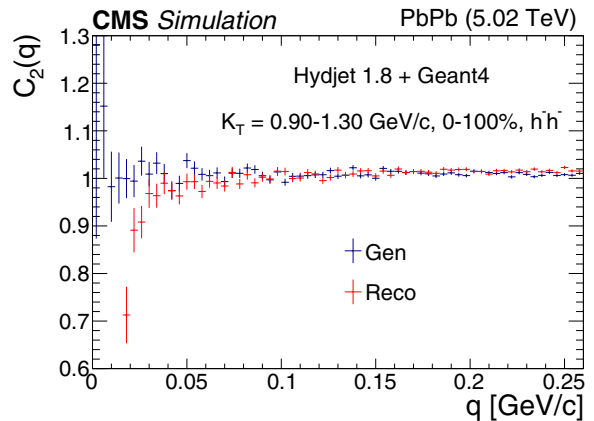


FIG. 3. The two-particle correlation function of negatively charged hadron pairs with $0.9 < K_T < 1.3 \text{ GeV}/c$ in the 0%–100% centrality range, calculated using Monte Carlo events with (Reco) and without (Gen) detector reconstruction effects. The error bars show the statistical uncertainties. The detector effects are most significant below approximately 50 MeV/c. The quantum-statistical effects are not present in the simulations, hence there is no Bose-Einstein peak.

TABLE I. The sources of the systematic uncertainties with their values in the default, lower, and upper settings. The meaning of the analysis parameters are given in Secs. IV A and IV B.

Systematic source	Default	Low	High
Vertex z selection	<15 cm	<12 cm	<18 cm
p_T selection	>0.5 GeV/ c	>0.55 GeV/ c	>0.5 GeV/ c
δp_T selection	<10%	<5%	<15%
$ \eta $ selection	<0.95	<0.9	<1
$N_{\text{pixel-hit}}$ selection	>1	>2	>0
$\chi^2 N_{\text{dof}}^{-1} N_{\text{layer}}$ selection	<0.18	<0.15	<0.18
$ d_{xy}/\sigma(d_{xy}) $ selection	<3	<2	<5
$ d_z/\sigma(d_z) $ selection	<3	<2	<5
$(\Delta\eta, \Delta\phi)$ pair selection	$\Delta\eta_{\min} = 0.014$ $\Delta\phi_{\min} = 0.022$	$\Delta\eta_{\min} = 0.017$ $\Delta\phi_{\min} = 0.028$	$\Delta\eta_{\min} = 0.011$ $\Delta\phi_{\min} = 0.016$
q_{\min} lower fit limit	$q_{\min}^0(K_T, \text{cent})$	$q_{\min}^0 - 0.004$	$q_{\min}^0 + 0.004$
q_{\max} upper fit limit	$q_{\max}^0(K_T, \text{cent})$	$0.85q_{\max}^0$	$1.15q_{\max}^0$
Centrality edges	Default values	Lower values	Higher values

limit ranging between 0.024 and 0.067 GeV/ c and the upper limit ranging between 0.12 and 0.55 GeV/ c . The limits were selected based on the confidence level and the convergence of the fit and based on the property of the Bose–Einstein peak, which moves towards higher q values for more peripheral collisions and as K_T increases.

E. Systematic uncertainties

The sources of systematic uncertainties considered in the analysis include the criteria for the event selection, the single-track selection, the pair-track selection, and the limits set on the fitted q range. Furthermore, the centrality calibration is also varied to estimate the systematic uncertainty resulting from this source. For each K_T and centrality class, the double-ratio correlation function $DR(q)$ was obtained and fitted with the nominal analysis parameters. Variations in the fit parameters were then determined by changing, individually, each of the analysis parameters to both its lowest and highest plausible values, and then fitting $DR(q)$ again using these values. The total systematic uncertainties were obtained by adding in quadrature all of the individual contributions for positive and negative modifications in the final fit parameters separately. Table I lists the analysis parameters and the range through which they were varied. These analysis parameters were separated into three categories. The “Track and event selection” category included the criteria on the z position of the vertex, the centrality edges, the selections of p_T , δp_T , $|\eta|$, $N_{\text{pixel-hit}}$, $|d_{xy}/\sigma(d_{xy})|$, and $|d_z/\sigma(d_z)|$, respectively. The “Pair selection” category included the $(\Delta\eta, \Delta\phi)$ pair selection. The “Fit limits” category included the q_{\min} lower, and the q_{\max} upper fit limits. The asymmetric systematic uncertainties for each of the fit parameters are summarized in Table II. Uncertainties for different K_T ranges and the two charge signs are averaged in each centrality range. For every fit parameter, the dominant systematic uncertainty results from the modification of the fit limits. The uncertainty corresponding to the pair selection criteria is highly asymmetric for the three most central cases, it is zero in one of the directions for all three parameters.

V. RESULTS

Three physical parameters (R , α , λ) were determined for each centrality and K_T class by fitting the theoretical formula to the measured correlation functions. The results are presented as a function of m_T . Systematic uncertainties are separated into correlated and uncorrelated point-to-point parts. Correlated uncertainties associate the same relative uncertainty for a given parameter for all centrality and K_T classes, whereas point-to-point values can vary between classes. This separation is necessary when investigating the m_T or centrality dependence of the fit parameters, where only the uncorrelated point-to-point uncertainty is used in determining the χ^2 values for the fits. The correlated part of the systematic uncertainty for each parameter value (R , λ , or α) is taken as the average uncertainty for the parameter. The point-to-point uncertainty for a parameter value is then the difference between the full systematic and the correlated uncertainties.

A. The Lévy scale parameter R

Figure 4 shows the R values obtained as a function of m_T . All values are found between 1.6 and 5.8 fm. The decreasing trend in m_T that is expected from hydrodynamics is observed. A clear centrality dependence is also visible. The decreasing value of R as collisions become more peripheral supports the geometric interpretation of this scale parameter.

To further analyze the m_T dependence of R , $1/R^2$ was plotted versus m_T as shown in Fig. 5. This plot is motivated by hydrodynamic predictions [11,12] that suggest a linear dependence when a Gaussian source is assumed. Here it is investigated whether a similar linear behavior exists for a Lévy source. Linear fits are shown in Fig. 5, with the fit parameters tabulated in Table III. Statistical and point-to-point systematic uncertainties were added in quadrature for the fits and used for the determination of the statistical uncertainties of the fit parameters. The confidence levels were statistically acceptable everywhere (i. e., have confidence level above 0.1%, similarly to Refs. [21,52]), suggesting that hydrodynamic scaling of $1/R^2$ holds for a Lévy source as well.

TABLE II. The relative effect of the different types of systematic sources in each centrality class for the R (upper Table), α (middle Table), and λ (lower Table) parameters (in percentage). The values were averaged over K_T and the two charge signs; the upwards (downwards) arrow, \uparrow (\downarrow) represents positive (negative) uncertainty in the value of the final fit parameters.

	Cent. [%]	Track and event selection		Pair selection		Fit limits		Overall	
		\uparrow	\downarrow	\uparrow	\downarrow	\uparrow	\downarrow	\uparrow	\downarrow
δR [%]	0–5	1.0	0.4	0.0	2.9	2.5	3.2	2.7	4.3
	5–10	0.7	0.5	0.0	2.1	2.0	2.3	2.1	3.2
	10–20	0.6	0.4	0.0	1.4	1.8	2.3	1.9	2.7
	20–30	0.6	0.3	0.2	1.6	1.8	1.9	1.9	2.5
	30–40	0.5	0.2	0.6	1.5	1.9	1.7	2.1	2.3
	40–60	0.5	0.5	0.7	1.4	1.9	1.7	2.1	2.3
$\delta\alpha$ [%]	0–5	0.6	0.7	4.8	0.0	6.9	3.8	8.4	3.9
	5–10	1.1	0.6	3.2	0.0	5.2	3.0	6.2	3.1
	10–20	0.3	0.4	1.9	0.0	4.9	3.0	5.3	3.0
	20–30	0.1	0.5	2.0	0.1	5.1	2.8	5.5	2.8
	30–40	0.2	0.7	2.0	0.7	4.5	3.5	4.9	3.6
	40–60	0.4	0.4	1.7	0.7	4.4	4.0	4.7	4.1
$\delta\lambda$ [%]	0–5	4.7	2.0	0.0	6.8	6.1	8.9	7.7	11.4
	5–10	3.7	1.7	0.0	5.5	4.9	6.9	6.1	9.0
	10–20	2.6	1.3	0.0	4.3	4.7	6.5	5.4	7.9
	20–30	2.4	1.0	1.1	4.4	4.2	6.4	5.0	7.8
	30–40	2.4	0.9	1.7	4.0	4.9	5.6	5.7	6.9
	40–60	2.0	0.9	1.7	3.3	5.6	5.1	6.2	6.1

The slope A and the intercept B of the linear fits are also related to hydrodynamic models. The slope A has a connection to the Hubble constant H of the quark-gluon plasma [12,61], with

$$A = \frac{H^2}{T_f}, \quad (14)$$

where T_f is the freeze-out temperature. With a Gaussian source assumption, the intercept B is related to the size of the

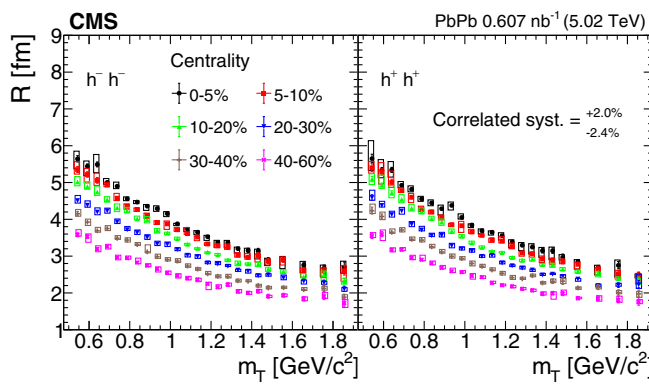


FIG. 4. The Lévy scale parameter R versus the transverse mass m_T in different centrality classes, for negatively (left) and positively (right) charged hadron pairs. The error bars show the statistical uncertainties, while the boxes indicate the point-to-point systematic uncertainties. These boxes are slightly shifted along the horizontal axes for better visibility. The correlated systematic uncertainty is also indicated.

source at freeze-out (R_f), with

$$R_f = \frac{1}{\sqrt{B}}. \quad (15)$$

Figure 6 shows that the slope parameter A has a strong centrality dependence, since the average number of nucleons participating in the collision ($\langle N_{\text{part}} \rangle$) is closely related to centrality. The mapping from a centrality class to $\langle N_{\text{part}} \rangle$ is given in Ref. [62]. By assuming a constant $T_f \approx 156$ MeV [63], the

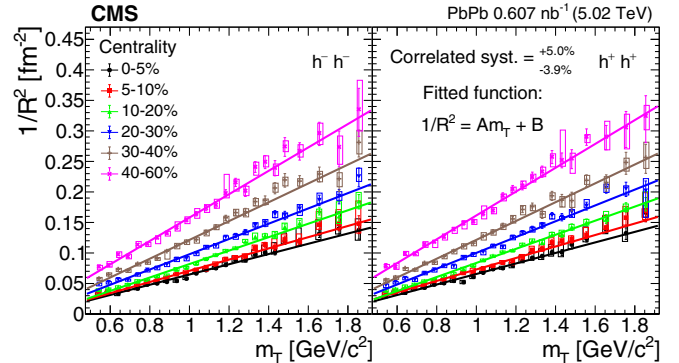


FIG. 5. The $1/R^2$ distribution vs transverse mass m_T in different centrality classes for negatively (left) and positively (right) charged hadron pairs. The error bars show the statistical uncertainties, while the boxes indicate the point-to-point systematic uncertainties. These boxes are slightly shifted along the horizontal axes for better visibility. The correlated systematic uncertainty is also indicated. A linear fit to the data is shown for each centrality bin. The fit parameters are tabulated in Table III.

TABLE III. Fit parameters and the corresponding confidence levels (CL) of the linear fits to $1/R^2$ versus m_T , for positively (left) and negatively (right) charged hadron pairs.

Cent. [%]	$h^+ h^+$			$h^- h^-$		
	$A [c^2 \text{ fm}^{-2} \text{ GeV}^{-1}]$	$B [\text{fm}^{-2}]$	CL [%]	$A [c^2 \text{ fm}^{-2} \text{ GeV}^{-1}]$	$B [\text{fm}^{-2}]$	CL [%]
0–5	0.086 ± 0.003	-0.021 ± 0.003	37.0	0.084 ± 0.002	-0.019 ± 0.002	10.5
5–10	0.094 ± 0.003	-0.021 ± 0.003	92.5	0.092 ± 0.003	-0.021 ± 0.002	78.1
10–20	0.115 ± 0.003	-0.032 ± 0.003	22.2	0.110 ± 0.002	-0.028 ± 0.002	1.0
20–30	0.130 ± 0.003	-0.029 ± 0.003	13.3	0.125 ± 0.003	-0.027 ± 0.003	23.2
30–40	0.154 ± 0.005	-0.033 ± 0.004	64.6	0.154 ± 0.004	-0.033 ± 0.004	6.2
40–60	0.195 ± 0.006	-0.034 ± 0.005	79.7	0.192 ± 0.006	-0.034 ± 0.005	82.7

value of the Hubble constant falls between 0.11 – 0.18 c/fm , from the most central to the most peripheral collisions. This indicates that the centrality of the collision affects the velocity of the expansion, resulting in larger velocities in more peripheral collisions. The values of the Hubble constant obtained here are close to the value of 0.17 c/fm measured in high-multiplicity proton-proton collisions at $\sqrt{s} = 13 \text{ TeV}$ [53], and are larger than the estimated value of 0.07 c/fm measured in 0% – 30% centrality AuAu collisions at $\sqrt{s_{\text{NN}}} = 200 \text{ GeV}$ [21]. The intercept parameter B is found to be negative in all cases (as shown in Fig. 6), which prevents a determination of the freeze-out size using Eq. (15). In the hydrodynamic models assuming a Gaussian shape, B is positive. The negative value found here might be related to the Lévy source assumed in the present analysis. Hydrodynamic solutions where B is negative are possible [64], although the implications for a Lévy source are not clear.

Figure 7 shows the dependence of R on $\langle N_{\text{part}} \rangle^{1/3}$ for eight representative samples of the 24 m_T classes considered in this analysis, where the source volume is expected to scale with $\langle N_{\text{part}} \rangle$. The results are fitted with a linear function for each m_T class. The fits are shown in Fig. 7, with the fit parameters and the corresponding confidence levels tabulated in Table IV. The

results are again consistent with a geometrical interpretation of the Lévy scale parameter R .

B. The Lévy stability index α

Figure 8 shows the values of α as a function of m_T for both negatively and positively charged hadron pairs. Within uncertainties, all values are found to fall in the range of 1.6 – 2.0 , with little m_T dependence within a given centrality class. However, there is a clear centrality dependence, with the results tending to a Gaussian shape ($\alpha = 2$) for the most central events. The observation that the correlation functions for some centralities can be described with Lévy functions having indices statistically inconsistent with a value of two means that a Gaussian assumption for the source shape is invalid in these cases. These Lévy distribution fits can be interpreted as suggesting the presence of anomalous diffusion resulting from expansion in the hadron gas. To more clearly show the centrality dependence, as well as the significance of the deviation from 2.0, Fig. 9 shows $\langle \alpha \rangle$ (the brackets indicating an average over m_T) as a function of $\langle N_{\text{part}} \rangle$ for both positively and negatively charged hadron pairs. A very similar linear dependence is observed for both charge signs.

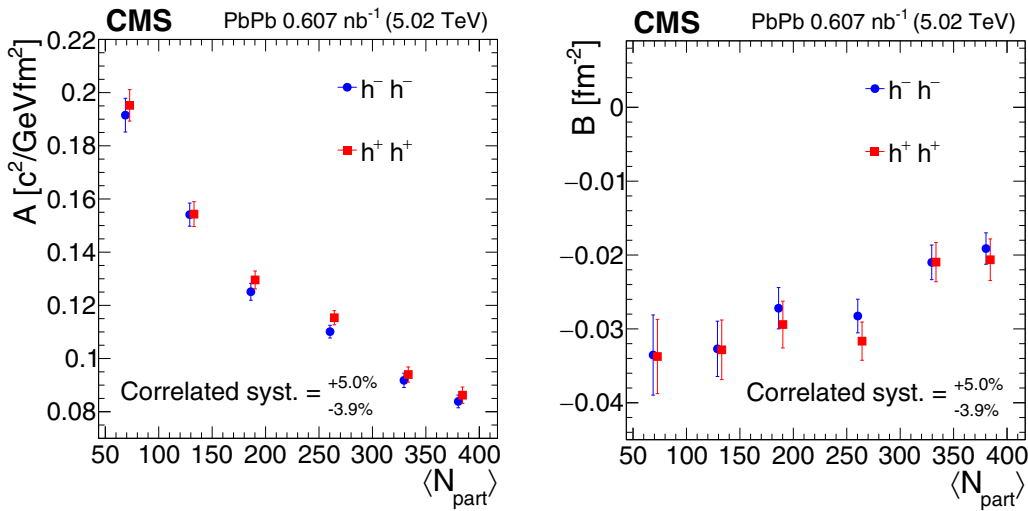


FIG. 6. The slope A (left) and the intercept B (right) linear-fit parameters versus $\langle N_{\text{part}} \rangle$ for positively and negatively charged hadron pairs. The error bars show the statistical uncertainties. The correlated systematic uncertainty is also indicated. The points are slightly shifted along the horizontal axes for better visibility.

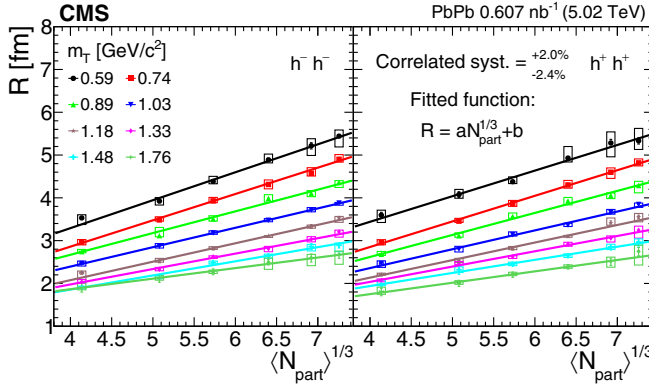


FIG. 7. The Lévy scale parameter R versus $\langle N_{\text{part}} \rangle^{1/3}$ in different m_T classes for negatively (left) and positively (right) charged hadron pairs. The error bars show the statistical uncertainties, while the boxes indicate the point-to-point systematic uncertainties. The correlated systematic uncertainty is also indicated. A linear fit to the data is shown for each m_T class. The fit parameters are tabulated in Table IV.

The PHENIX Collaboration at RHIC reported a mean value for α of 1.207 for pions pairs with $|\eta| < 0.35$ and $228 < m_T < 871 \text{ MeV}/c^2$ in 0%–30% centrality AuAu collisions at $\sqrt{s_{\text{NN}}} = 200 \text{ GeV}$ [21]. Very little m_T dependence was observed at RHIC, a result similar to that reported here. However, our value for $\langle \alpha \rangle$ in the same centrality range is 45%–60% larger. This increase in the Lévy stability index may be connected to the larger energy densities achieved at the CERN Large Hadron Collider (LHC), which would be expected to result in less anomalous diffusion. An increasing energy density could also explain the increase of $\langle \alpha \rangle$ with $\langle N_{\text{part}} \rangle$.

C. The correlation strength λ

The measured λ values are shown in Fig. 10 as a function of m_T , for both negatively and positively charged hadron pairs. The values decrease with increasing transverse mass and as the collisions become more central.

The value of λ is reduced compared with the case of using identified pions only, because the sample contains particles other than pions (mostly kaons and protons). The strength of

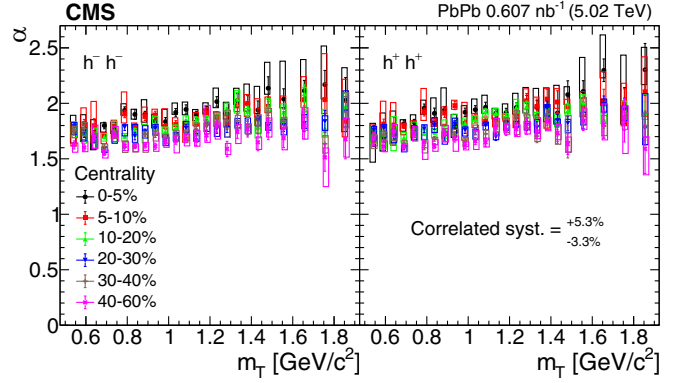


FIG. 8. The Lévy stability index α versus the transverse mass m_T in different centrality classes, for negatively (left) and positively (right) charged hadron pairs. The error bars show the statistical uncertainties, while the boxes indicate the point-to-point systematic uncertainties. These boxes are slightly shifted along the horizontal axes for better visibility. The correlated systematic uncertainty is also indicated.

the correlation is proportional to the number of identical pion pairs, and pairs of nonidentical particles decrease the observed correlation. To see how the lack of particle identification affects the value of λ , a new parameter λ^* is introduced by rescaling λ with the square of the pion fraction:

$$\lambda^* = \frac{\lambda}{(N_{\text{pion}}/N_{\text{hadron}})^2}. \quad (16)$$

The centrality and K_T dependent pion fraction was measured by the ALICE Collaboration in the range $|\eta| < 0.5$, as reported in Ref. [51]. The calculated λ^* values as a function of m_T are shown in Fig. 10. In each of the centrality classes and m_T bins, λ^* is smaller than 1, which indicates that there exist additional effects lowering the correlation strength beyond the lack of particle identification discussed above. This result of $\lambda^* < 1$ can, in fact, be understood on the basis of the core-halo model. In this interpretation, λ^* describes the square of the fraction of pions produced in the core, as detailed in Eqs. (4) and (5). Furthermore, λ^* is found to lack any clear m_T dependence for a given centrality class. This is consistent with the observations at RHIC [21] and can be explained in

TABLE IV. Fit parameters and the corresponding confidence levels (CL) of the linear fits to R versus $\langle N_{\text{part}} \rangle^{1/3}$ for positively (left) and negatively (right) charged hadron pairs.

m_T [GeV/ c^2]	$h^+ h^+$			$h^- h^-$		
	a [fm]	b [fm]	CL [%]	a [fm]	b [fm]	CL [%]
0.59	0.60 ± 0.08	1.05 ± 0.44	88.1	0.65 ± 0.06	0.68 ± 0.35	79.5
0.74	0.60 ± 0.03	0.46 ± 0.15	96.1	0.62 ± 0.03	0.40 ± 0.17	90.7
0.89	0.51 ± 0.03	0.56 ± 0.18	56.0	0.51 ± 0.02	0.64 ± 0.12	70.8
1.03	0.44 ± 0.03	0.60 ± 0.18	69.0	0.45 ± 0.02	0.58 ± 0.15	99.8
1.18	0.41 ± 0.02	0.49 ± 0.11	54.5	0.43 ± 0.04	0.35 ± 0.23	94.0
1.33	0.36 ± 0.03	0.61 ± 0.16	84.0	0.36 ± 0.03	0.54 ± 0.14	92.0
1.48	0.31 ± 0.03	0.71 ± 0.18	96.3	0.33 ± 0.03	0.53 ± 0.16	64.2
1.76	0.27 ± 0.04	0.69 ± 0.26	98.9	0.25 ± 0.06	0.88 ± 0.32	99.9

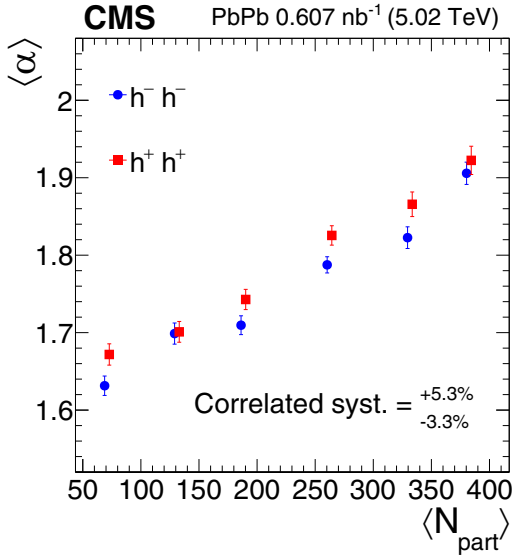


FIG. 9. The average Lévy stability index $\langle \alpha \rangle$ versus $\langle N_{\text{part}} \rangle$, for both positively and negatively charged hadron pairs. The error bars show the statistical uncertainties. The correlated systematic uncertainty is also indicated. The points are slightly shifted along the horizontal axes for better visibility.

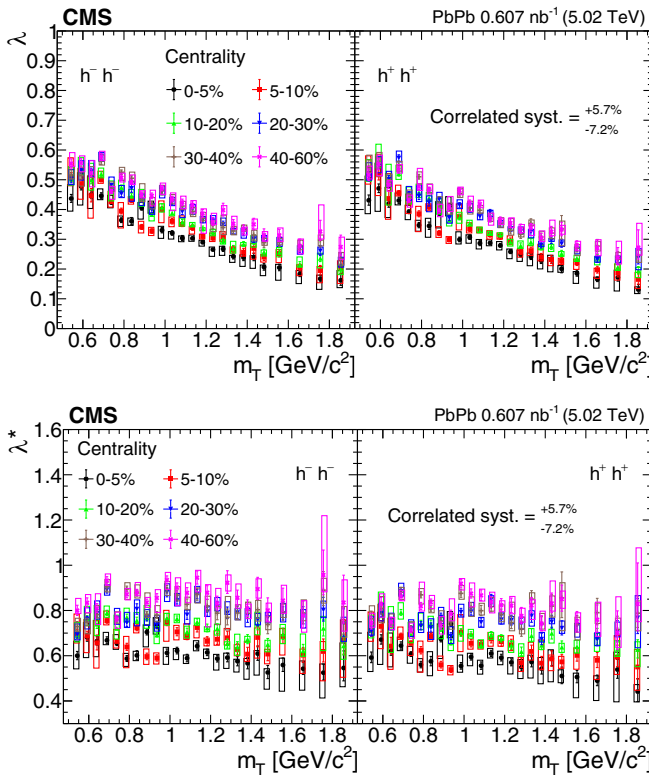


FIG. 10. The correlation strength λ (upper panel) and λ^* , which is rescaled with the square of the pion fraction (lower panel), versus the transverse mass m_T in different centrality classes, for negatively (left) and positively (right) charged hadron pairs. The error bars show the statistical uncertainties, while the boxes indicate the point-to-point systematic uncertainties. These boxes are slightly shifted along the horizontal axes for better visibility. The correlated systematic uncertainty is also indicated.

terms of the core-halo model by the negligible momentum dependence of the core fraction in the investigated range. The decrease in λ^* with centrality suggests a relatively smaller halo contribution for peripheral collisions.

VI. SUMMARY

Two-particle Bose–Einstein momentum correlation function measurements are presented. The data sample consists of 4.27×10^9 minimum bias lead-lead (PbPb) events, corresponding to an integrated luminosity of 0.607 nb^{-1} , at a center-of-mass energy per nucleon pair of $\sqrt{s_{\text{NN}}} = 5.02 \text{ TeV}$, recorded by the CMS experiment at the LHC. The correlation functions found in different centrality and average transverse momentum classes are analyzed in terms of Lévy sources, including Coulomb effects. The values of the Lévy scale parameter R , the Lévy stability index α , and the correlation strength λ are determined.

A geometric interpretation of the R parameter is suggested by its dependence on the average number of participating nucleons in the collision. Assuming a pion mass for the charged particles, a linear dependence of $1/R^2$ on the transverse mass (m_T) is observed, consistent with a hydrodynamic scaling behavior, even for the case of Lévy sources. Based on the observed linear behavior, it is estimated that the Hubble constant of the quark-gluon plasma created in 5.02 TeV PbPb collisions increases from 0.11 c/fm to 0.18 c/fm when moving from most central to most peripheral collisions. The intercept of the $1/R^2$ versus m_T linear fits is negative in all cases, requiring further studies for its interpretation. The α parameter is found to have little, if any, m_T dependence and to range between 1.6–2.0, increasing with centrality. The α values found in this paper are approximately 45%–60% larger than those reported for gold-gold collisions at $\sqrt{s_{\text{NN}}} = 200 \text{ GeV}$ at RHIC. This increase, while not fully understood, may result from the greater energy densities achieved at the LHC. As a function of m_T , a strong and decreasing trend is observed for the λ parameter, which can be explained by the lack of particle identification. After rescaling the λ values to account for the fraction of pions among the charged hadrons, a nearly constant trend of the pion-fraction-corrected λ^* with m_T is observed. The λ^* values are found to be smaller than unity, which can be interpreted on the basis of the core-halo model as a non-negligible halo contribution. Furthermore, λ^* is found to decrease as the collisions become more central. Altogether, these results imply that the hadron emitting source in $\sqrt{s_{\text{NN}}} = 5.02 \text{ TeV}$ PbPb collisions can be described by Lévy distributions. This allows for a new and precise characterization of this source in high-energy heavy ion collisions.

ACKNOWLEDGMENTS

We congratulate our colleagues in the CERN accelerator departments for the excellent performance of the LHC and thank the technical and administrative staffs at CERN and at other CMS institutes for their contributions to the success of the CMS effort. In addition, we gratefully acknowledge the computing centers and personnel of the Worldwide LHC Computing Grid and other centers for delivering so

effectively the computing infrastructure essential to our analyses. Finally, we acknowledge the enduring support for the construction and operation of the LHC, the CMS detector, and the supporting computing infrastructure provided by the following funding agencies: BMBWF and FWF (Austria); FNRS and FWO (Belgium); CNPq, CAPES, FAPERJ, FAPERGS, and FAPESP (Brazil); MES and BNSF (Bulgaria); CERN; CAS, MoST, and NSFC (China); MINCIENCIAS (Colombia); MSES and CSF (Croatia); RIF (Cyprus); SENESCYT (Ecuador); MoER, ERC PUT and ERDF (Estonia); Academy of Finland, MEC, and HIP (Finland); CEA and CNRS/IN2P3 (France); BMBF, DFG, and HGF (Germany); GSRI (Greece); NKFIH (Hungary); DAE and DST (India); IPM (Iran); SFI (Ireland); INFN (Italy); MSIP and NRF (Republic of Korea); MES (Latvia); LAS (Lithuania); MOE and UM (Malaysia); BUAP, CINVESTAV, CONACYT, LNS, SEP, and UASLP-FAI (Mexico); MOS (Montenegro); MBIE (New Zealand); PAEC (Pakistan); MES and NSC (Poland); FCT (Portugal); MESTD (Serbia); MCIN/AEI and PCTI (Spain); MOSTR (Sri Lanka); Swiss Funding Agencies (Switzerland); MST (Taipei); MHESI and NSTDA (Thailand); TUBITAK and TENMAK (Turkey); NASU (Ukraine); STFC (United Kingdom); DOE and NSF (USA).

Individuals have received support from the Marie-Curie program and the European Research Council and Horizon 2020 Grant, Contracts No. 675440, No. 724704, No. 752730, No. 758316, No. 765710, No. 824093, and No. 884104, and COST Action CA16108 (European Union); the Leventis Foundation; the Alfred P. Sloan Foundation; the Alexander von Humboldt Foundation; the Belgian Federal Science Policy Office; the Fonds pour la Formation à la Recherche dans l'Industrie et dans l'Agriculture (FRIA-Belgium); the Agentschap voor Innovatie door Wetenschap en Technologie (IWT-Belgium); the F. R.S.-FNRS and FWO (Belgium)

under the “Excellence of Science—EOS”—be.h Project No. 30820817; the Beijing Municipal Science & Technology Commission, No. Z191100007219010; the Ministry of Education, Youth and Sports (MEYS) of the Czech Republic; the Hellenic Foundation for Research and Innovation (HFRI), Project No. 2288 (Greece); the Deutsche Forschungsgemeinschaft (DFG), under Germany’s Excellence Strategy—EXC 2121 “Quantum Universe”—390833306, and under Project No. 400140256 - GRK2497; the Hungarian Academy of Sciences, the New National Excellence Program - UNKP, the NKFIH research grants K 124845, K 124850, K 128713, K 128786, K 129058, K 131991, K 133046, K 138136, K 143460, K 143477, 2020-2.2.1-ED-2021-00181, and TKP2021-NKTA-64 (Hungary); the Council of Science and Industrial Research, India; the Latvian Council of Science; the Ministry of Education and Science, Project no. 2022/WK/14, and the National Science Center, contracts Opus 2021/41/B/ST2/01369 and 2021/43/B/ST2/01552 (Poland); the Fundação para a Ciência e a Tecnologia, Grant No. CEECIND/01334/2018 (Portugal); the National Priorities Research Program by Qatar National Research Fund; MCIN/AEI/10.13039/501100011033, ERDF “a way of making Europe,” and the Programa Estatal de Fomento de la Investigación Científica y Técnica de Excelencia María de Maeztu, Grant No. MDM-2017-0765 and Programa Severo Ochoa del Principado de Asturias (Spain); the Chulalongkorn Academic into its second Century Project Advancement Project, and the National Science, Research and Innovation Fund via the Program Management Unit for Human Resources & Institutional Development, Research and Innovation, Grant No. B05F650021 (Thailand); the Kavli Foundation; the Nvidia Corporation; the SuperMicro Corporation; the Welch Foundation, Contract No. C-1845; and the Weston Havens Foundation (USA).

-
- [1] G. Goldhaber, W. B. Fowler, S. Goldhaber, and T. F. Hoang, Pion-pion correlations in antiproton annihilation events, *Phys. Rev. Lett.* **3**, 181 (1959).
 - [2] G. Goldhaber, S. Goldhaber, W.-Y. Lee, and A. Pais, Influence of Bose-Einstein statistics on the antiproton proton annihilation process, *Phys. Rev.* **120**, 300 (1960).
 - [3] R. J. Glauber, Photon correlations, *Phys. Rev. Lett.* **10**, 84 (1963).
 - [4] R. J. Glauber, Nobel lecture: One hundred years of light quanta, *Rev. Mod. Phys.* **78**, 1267 (2006).
 - [5] R. J. Glauber, Quantum optics and heavy ion physics, in *Proceedings, 18th International Conference on Ultra-Relativistic Nucleus-Nucleus Collisions (Quark Matter 2005): Budapest, Hungary, August 4-9, 2005*, *Nucl. Phys. A* **774**, 3 (2006).
 - [6] R. Hanbury Brown and R. Q. Twiss, A test of a new type of stellar interferometer on Sirius, *Nature (London)* **178**, 1046 (1956).
 - [7] R. Lednicky, Femtoscopy with unlike particles, in *International Workshop on the Physics of the Quark Gluon Plasma (2001)*, arXiv:nucl-th/0112011.
 - [8] S. S. Adler *et al.* (PHENIX Collaboration), Bose-Einstein correlations of charged pion pairs in Au+Au collisions at $\sqrt{s_{NN}} = 200 \text{ GeV}$, *Phys. Rev. Lett.* **93**, 152302 (2004).
 - [9] I. G. Bearden *et al.* (NA44 Collaboration), Two kaon correlations in central Pb+Pb collisions at 158A GeV/c, *Phys. Rev. Lett.* **87**, 112301 (2001).
 - [10] S. Afanasiev *et al.* (PHENIX Collaboration), Kaon interferometric probes of space-time evolution in Au+Au collisions at $\sqrt{s_{NN}} = 200 \text{ GeV}$, *Phys. Rev. Lett.* **103**, 142301 (2009).
 - [11] A. N. Makhlin and Y. M. Sinyukov, Hydrodynamics of hadron matter under pion interferometric microscope, *Z. Phys. C: Part. Fields* **39**, 69 (1988).
 - [12] T. Csörgő and B. Lörstad, Bose-Einstein correlations for three-dimensionally expanding, cylindrically symmetric, finite systems, *Phys. Rev. C* **54**, 1390 (1996).
 - [13] M. Csanád, T. Csörgő, B. Lörstad, and A. Ster, Indication of quark deconfinement and evidence for a bubble flow in 130 GeV and 200 GeV Au+Au collisions, *J. Phys. G* **30**, S1079 (2004).
 - [14] S. Pratt, Resolving the HBT puzzle in relativistic heavy ion collision, *Phys. Rev. Lett.* **102**, 232301 (2009).
 - [15] R. A. Lacey, Indications for a critical end point in the phase diagram for hot and dense nuclear matter, *Phys. Rev. Lett.* **114**, 142301 (2015).
 - [16] J. Adams *et al.* (STAR Collaboration), Pion interferometry in Au+Au collisions at $\sqrt{s_{NN}} = 200 \text{ GeV}$, *Phys. Rev. C* **71**, 044906 (2005).

- [17] ALICE Collaboration, One-dimensional pion, kaon, and proton femtoscopy in Pb-Pb collisions at $\sqrt{s_{NN}} = 2.76$ TeV, *Phys. Rev. C* **92**, 054908 (2015).
- [18] ALICE Collaboration, Centrality dependence of pion freeze-out radii in Pb-Pb collisions at $\sqrt{s_{NN}} = 2.76$ TeV, *Phys. Rev. C* **93**, 024905 (2016).
- [19] CMS Collaboration, Bose-Einstein correlations in pp , $p\text{Pb}$, and PbPb collisions at $\sqrt{s_{NN}} = 0.9\text{--}7$ TeV, *Phys. Rev. C* **97**, 064912 (2018).
- [20] ATLAS Collaboration, Femtoscopy with identified charged pions in proton-lead collisions at $\sqrt{s_{NN}} = 5.02$ TeV with ATLAS, *Phys. Rev. C* **96**, 064908 (2017).
- [21] A. Adare *et al.* (PHENIX Collaboration), Lévy-stable two-pion Bose-Einstein correlations in $\sqrt{s_{NN}} = 200$ GeV Au+Au collisions, *Phys. Rev. C* **97**, 064911 (2018).
- [22] H. Adhikary *et al.* (NA61/SHINE Collaboration), Measurements of two-pion HBT correlations in Be+Be collisions at 150A GeV/c beam momentum, at the NA61/SHINE experiment at CERN, *Eur. Phys. J. C* **83**, 919 (2023).
- [23] V. V. Uchaikin and V. M. Zolotarev, *Chance and Stability: Stable Distributions and Their Applications* (De Gruyter, Berlin, Boston, 1999).
- [24] T. Csörgő, S. Hegyi, T. Novák, and W. A. Zajc, Bose-Einstein or HBT correlations and the anomalous dimension of QCD, *Acta Phys. Pol. B* **36**, 329 (2005).
- [25] T. Csörgő, S. Hegyi, T. Novák, and W. A. Zajc, Bose-Einstein or HBT correlation signature of a second order QCD phase transition, *AIP Conf. Proc.* **828**, 525 (2006).
- [26] M. Csanád, T. Csörgő, and M. Nagy, Anomalous diffusion of pions at RHIC, *Braz. J. Phys.* **37**, 1002 (2007).
- [27] D. Kincses, M. Stefaniak, and M. Csanád, Event-by-event investigation of the two-particle source function in heavy-ion collisions with EPOS, *Entropy* **24**, 308 (2022).
- [28] B. Kórodi, D. Kincses, and M. Csanád, Event-by-event investigation of the two-particle source function in $\sqrt{s_{NN}} = 2.76$ TeV PbPb collisions with EPOS, *Phys. Lett. B* **847**, 138295 (2023).
- [29] HEPData record for this analysis (2023).
- [30] T. Csörgő, Particle interferometry from 40 MeV to 40 TeV, *Acta Phys. Hung. New Ser.: Heavy Ion Phys.* **15**, 1 (2002).
- [31] U. A. Wiedemann and U. W. Heinz, Particle interferometry for relativistic heavy ion collisions, *Phys. Rep.* **319**, 145 (1999).
- [32] J. Bolz, U. Ornik, M. Plumer, B. R. Schlei, and R. M. Weiner, Resonance decays and partial coherence in Bose-Einstein correlations, *Phys. Rev. D* **47**, 3860 (1993).
- [33] T. Csörgő, B. Lörstad, and J. Zimányi, Bose-Einstein correlations for systems with large halo, *Z. Phys. C: Part. Fields* **71**, 491 (1996).
- [34] A. Kisiel, W. Florkowski, W. Broniowski, and J. Pluta, Femtoscopy in hydro-inspired models with resonances, *Phys. Rev. C* **73**, 064902 (2006).
- [35] ALICE Collaboration, Search for a common baryon source in high-multiplicity pp collisions at the LHC, *Phys. Lett. B* **811**, 135849 (2020).
- [36] D. Mihaylov and J. González González, Novel model for particle emission in small collision systems, *Eur. Phys. J. C* **83**, 590 (2023).
- [37] R. Metzler, E. Barkai, and J. Klafter, Anomalous diffusion and relaxation close to thermal equilibrium: A fractional Fokker-Planck equation approach, *Phys. Rev. Lett.* **82**, 3563 (1999).
- [38] T. Csörgő, S. Hegyi, and W. A. Zajc, Bose-Einstein correlations for Lévy stable source distributions, *Eur. Phys. J. C* **36**, 67 (2004).
- [39] Y. Sinyukov, R. Lednický, S. V. Akkelin, J. Pluta, and B. Erazmus, Coulomb corrections for interferometry analysis of expanding hadron systems, *Phys. Lett. B* **432**, 248 (1998).
- [40] M. Csanád, S. Lökö, and M. Nagy, Expanded empirical formula for Coulomb final state interaction in the presence of Lévy sources, *Phys. Part. Nucl.* **51**, 238 (2020).
- [41] W. Adam *et al.* (CMS Tracker Group), The CMS phase-1 pixel detector upgrade, *J. Instrum.* **2021**, P02027 (2021).
- [42] CMS Collaboration, *Track Impact Parameter Resolution for the Full Pseudo Rapidity Coverage in the 2017 Dataset with the CMS Phase-1 Pixel Detector*, CMS Detector Performance Note CMS-DP-2020-049 (2020).
- [43] CMS Collaboration, The CMS trigger system, *J. Instrum.* **12**, P01020 (2017).
- [44] CMS Collaboration, The CMS experiment at the CERN LHC, *J. Instrum.* **3**, S08004 (2008).
- [45] CMS Collaboration, Precision luminosity measurement in proton-proton collisions at $\sqrt{s} = 13$ TeV in 2015 and 2016 at CMS, *Eur. Phys. J. C* **81**, 800 (2021).
- [46] CMS Collaboration, CMS Luminosity Measurement using Nucleus-Nucleus Collisions at $\sqrt{s_{NN}} = 5.02$ TeV in 2018, CMS Physics Analysis Summary CMS-PAS-LUM-18-001 (2022), <https://cds.cern.ch/record/2809613>.
- [47] CMS Collaboration, Charged-particle nuclear modification factors in PbPb and $p\text{Pb}$ collisions at $\sqrt{s_{NN}} = 5.02$ TeV, *J. High Energy Phys.* **04** (2017) 039.
- [48] CMS Collaboration, Observation and studies of jet quenching in PbPb collisions at $\sqrt{s_{NN}} = 2.76$ TeV, *Phys. Rev. C* **84**, 024906 (2011).
- [49] CMS Collaboration, Description and performance of track and primary-vertex reconstruction with the CMS tracker, *J. Instrum.* **9**, P10009 (2014).
- [50] M. Csanád, T. Csörgő, B. Lörstad, and A. Ster, Understanding the rapidity dependence of the elliptic flow and the HBT radii at RHIC, *AIP Conf. Proc.* **828**, 479 (2006).
- [51] ALICE Collaboration, Production of charged pions, kaons, and (anti-)protons in Pb-Pb and inelastic pp collisions at $\sqrt{s_{NN}} = 5.02$ TeV, *Phys. Rev. C* **101**, 044907 (2020).
- [52] P. Achard *et al.* (L3 Collaboration), Test of the τ -model of Bose-Einstein correlations and reconstruction of the source function in hadronic Z-boson decay at LEP, *Eur. Phys. J. C* **71**, 1648 (2011).
- [53] CMS Collaboration, Bose-Einstein correlations of charged hadrons in proton-proton collisions at $\sqrt{s} = 13$ TeV, *J. High Energy Phys.* **03** (2020) 014.
- [54] B. Kurylis, D. Kincses, M. Nagy, and M. Csanád, Coulomb interaction for Lévy sources, *Universe* **9**, 328 (2023).
- [55] CMS Collaboration, K_S^0 and $\lambda(\bar{\lambda})$ two-particle femtoscopic correlations in PbPb collisions at $\sqrt{s_{NN}} = 5.02$ TeV, [arXiv:2301.05290](https://arxiv.org/abs/2301.05290).
- [56] F. James and M. Roos, Minuit: A system for function minimization and analysis of the parameter errors and correlations, *Comput. Phys. Commun.* **10**, 343 (1975).
- [57] R. Brun and F. Rademakers, ROOT: An object oriented data analysis framework, *Nucl. Instrum. Methods Phys. Res., Sect. A* **389**, 81 (1997).

- [58] I. P. Lohkhtin and A. M. Snigirev, A model of jet quenching in ultrarelativistic heavy ion collisions and high- p_T hadron spectra at RHIC, *Eur. Phys. J. C* **45**, 211 (2006).
- [59] S. Agostinelli *et al.* (GEANT4 Collaboration), GEANT4—a simulation toolkit, *Nucl. Instrum. Methods Phys. Res., Sect. A* **506**, 250 (2003).
- [60] D. Kincses, M. I. Nagy, and M. Csanad, Coulomb and strong interactions in the final state of Hanbury-Brown-Twiss correlations for Levy-type source functions, *Phys. Rev. C* **102**, 064912 (2020).
- [61] M. Chojnacki, W. Florkowski, and T. Csorgo, On the formation of Hubble flow in little bangs, *Phys. Rev. C* **71**, 044902 (2005).
- [62] C. Loizides, J. Kamin, and D. d’Enterria, Improved Monte Carlo Glauber predictions at present and future nuclear colliders, *Phys. Rev. C* **97**, 054910 (2018).
- [63] P. Steinbrecher (HotQCD Collaboration), The QCD crossover at zero and non-zero baryon densities from lattice QCD, *Nucl. Phys. A* **982**, 847 (2019).
- [64] T. Csorgo, Simple analytic solution of fireball hydrodynamics, *Central Eur. J. Phys.* **2**, 556 (2004).

- A. Tumasyan^{1,a}, W. Adam², J. W. Andrejkovic,² T. Bergauer², S. Chatterjee², K. Damanakis², M. Dragicevic², A. Escalante Del Valle², P. S. Hussain², M. Jeitler², N. Krammer², L. Lechner², D. Liko², I. Mikulec², P. Paulitsch,² J. Schieck², R. Schofbeck², D. Schwarz², M. Sonawane², S. Templ², W. Waltenberger², C.-E. Wulz², M. R. Darwish^{3,c}, T. Janssen³, T. Kello,^{3,d} H. Rejeb Sfar,³ P. Van Mechelen³, E. S. Bols⁴, J. D’Hondt⁴, A. De Moor⁴, M. Delcourt⁴, H. El Faham⁴, S. Lowette⁴, A. Morton⁴, D. Mller⁴, A. R. Sahasransu⁴, S. Tavernier⁴, W. Van Doninck,⁴ S. Van Putte⁴, D. Vannerom⁴, B. Clerbaux⁵, S. Dansana⁵, G. De Lentdecker⁵, L. Favart⁵, D. Hohov⁵, J. Jaramillo⁵, K. Lee⁵, M. Mahdavikhorrami⁵, I. Makarenko⁵, A. Malara⁵, S. Paredes⁵, L. Ptre⁵, N. Postiau,⁵ L. Thomas⁵, M. Vanden Bemden,⁵ C. Vander Velde⁵, P. Vanlaer⁵, D. Dobur⁶, J. Knolle⁶, L. Lambrecht⁶, G. Mestdach,⁶ C. Rendon,⁶ A. Samalan,⁶ K. Skovpen⁶, M. Tytgat⁶, N. Van Den Bossche⁶, B. Vermassen,⁶ L. Wezenbeek⁶, A. Benecke⁷, G. Bruno⁷, F. Fury⁷, C. Caputo⁷, P. David⁷, C. Delaere⁷, I. S. Donertas⁷, A. Giannanco⁷, K. Jaffel⁷, Sa. Jain⁷, V. Lemaitre,⁷ K. Mondal⁷, A. Taliercio⁷, T. T. Tran⁷, P. Vischia⁷, S. Wertz⁷, G. A. Alves⁸, E. Coelho⁸, C. Hensel⁸, A. Moraes⁸, P. Rebello Teles⁸, W. L. Alda Jnior⁹, M. Alves Gallo Pereira⁹, M. Barroso Ferreira Filho⁹, H. Brandao Malbouisson⁹, W. Carvalho⁹, J. Chinellato,^{9,e} E. M. Da Costa⁹, G. G. Da Silveira^{9,f}, D. De Jesus Damiao⁹, V. Dos Santos Sousa⁹, S. Fonseca De Souza⁹, J. Martins^{9,g}, C. Mora Herrera⁹, K. Mota Amarilo⁹, L. Mundim⁹, H. Nogima⁹, A. Santoro⁹, S. M. Silva Do Amaral⁹, A. Sznajder⁹, M. Thiel⁹, A. Vilela Pereira⁹, C. A. Bernardes^{10,f}, L. Calligaris¹⁰, T. R. Fernandez Perez Tomei¹⁰, E. M. Gregores¹⁰, P. G. Mercadante¹⁰, S. F. Novaes¹⁰, Sandra S. Padula¹⁰, A. Aleksandrov¹¹, G. Antchev¹¹, R. Hadjiiska¹¹, P. Iaydjiev¹¹, M. Misheva¹¹, M. Rodozov,¹¹ M. Shopova¹¹, G. Sultanov¹¹, A. Dimitrov¹², T. Ivanov¹², L. Litov¹², B. Pavlov¹², P. Petkov¹², A. Petrov¹², E. Shumka¹², S. Thakur¹³, T. Cheng¹⁴, T. Javaid^{14,h}, M. Mittal¹⁴, L. Yuan¹⁴, M. Ahmad¹⁵, G. Bauer,^{15,i} Z. Hu¹⁵, S. Lezki¹⁵, K. Yi^{15,i,j}, G. M. Chen¹⁶, H. S. Chen^{16,h}, M. Chen^{16,h}, F. Iemmi¹⁶, C. H. Jiang,¹⁶ A. Kapoor¹⁶, H. Liao¹⁶, Z.-A. Liu^{16,h}, V. Milosevic¹⁶, F. Monti¹⁶, R. Sharma¹⁶, J. Tao¹⁶, J. Thomas-Wilsker¹⁶, J. Wang¹⁶, H. Zhang¹⁶, J. Zhao¹⁶, A. Agapitos¹⁷, Y. An¹⁷, Y. Ban¹⁷, A. Levin¹⁷, C. Li¹⁷, Q. Li¹⁷, X. Lyu,¹⁷ Y. Mao,¹⁷, S. J. Qian¹⁷, X. Sun¹⁷, D. Wang¹⁷, J. Xiao¹⁷, H. Yang,¹⁷, M. Lu¹⁸, Z. You¹⁸, N. Lu¹⁹, X. Gao^{20,d}, D. Leggat,²⁰ H. Okawa²⁰, Y. Zhang²⁰, Z. Lin²¹, C. Lu²¹, M. Xiao²¹, C. Avila²², D. A. Barbosa Trujillo,²² A. Cabrera²², C. Florez²², J. Fraga²², J. Mejia Guisao²³, F. Ramirez²³, M. Rodriguez²³, J. D. Ruiz Alvarez²³, D. Giljanovic²⁴, N. Godinovic²⁴, D. Lelas²⁴, I. Puljak²⁴, Z. Antunovic,²⁵ M. Kovac²⁵, T. Sculac²⁵, V. Brigljevic²⁶, B. K. Chitroda²⁶, D. Ferencek²⁶, S. Mishra²⁶, M. Roguljic²⁶, A. Starodumov^{26,k}, T. Susa²⁶, A. Attikis²⁷, K. Christoforou²⁷, S. Konstantinou²⁷, J. Mousa²⁷, C. Nicolaou²⁷, F. Ptochos²⁷, P. A. Razis²⁷, H. Rykaczewski²⁷, H. Saka²⁷, A. Stepennov²⁷, M. Finger^{28,k}, M. Finger, Jr.^{28,k}, A. Kveton²⁸, E. Ayala²⁹, E. Carrera Jarrin³⁰, H. Abdalla^{31,l}, Y. Assran,^{31,m,n}, M. Abdullah Al-Mashad³², M. A. Mahmoud³², S. Bhowmik³³, R. K. Dewanjee³³, K. Ehatahta³³, M. Kadastik,³³ T. Lange³³, S. Nandan³³, C. Nielsen³³, J. Pata³³, M. Raidal³³, L. Tani³³, C. Veelken³³, P. Eerola³⁴, H. Kirschenmann³⁴, K. Osterberg³⁴, M. Voutilainen³⁴, S. Bharthuar³⁵, E. Brcken³⁵, F. Garcia³⁵, J. Havukainen³⁵, M. S. Kim³⁵, R. Kinnunen³⁵, T. Lampn³⁵, K. Lassila-Perini³⁵, S. Lehti³⁵, T. Lindn³⁵, M. Lotti,³⁵ L. Martikainen³⁵, M. Myllymaki³⁵, M. m. Rantanen³⁵, H. Siikonen³⁵, E. Tuominen³⁵, J. Tuominiemi³⁵, P. Luukka³⁶, H. Petrow³⁶, T. Tuuva,^{36,o} C. Amendola³⁷, M. Besancon³⁷, F. Couderc³⁷, M. Dejardin³⁷, D. Denegri,³⁷ J. L. Faure,³⁷ F. Ferri³⁷, S. Ganjour³⁷, P. Gras³⁷, G. Hamel de Monchenault³⁷, V. Lohezic³⁷, J. Malcles³⁷, J. Rander,³⁷ A. Rosowsky³⁷, M. . Sahin³⁷, A. Savoy-Navarro^{37,p}, P. Simkina³⁷, M. Titov³⁷, C. Baldenegro Barrera³⁸, F. Beaudette³⁸, A. Buchot Perraguin³⁸, P. Busson³⁸, A. Cappati³⁸, C. Charlot³⁸, F. Damas³⁸, O. Davignon³⁸, B. Diab³⁸, G. Falmagne³⁸, B. A. Fontana Santos Alves³⁸, S. Ghosh³⁸, R. Granier de Cassagnac³⁸, A. Hakimi³⁸, B. Harikrishnan³⁸, G. Liu³⁸, J. Motta³⁸, M. Nguyen³⁸, C. Ochando³⁸, L. Portales³⁸, R. Salerno³⁸, U. Sarkar³⁸, J. B. Sauvan³⁸, Y. Sirois³⁸, A. Tarabini³⁸, E. Vernazza³⁸, A. Zabi³⁸, A. Zghiche³⁸, J.-L. Agram^{39,q}, J. Andrea³⁹, D. Apparau³⁹, D. Bloch³⁹, G. Bourgat³⁹, J.-M. Brom³⁹, E. C. Chabert³⁹, C. Collard³⁹, D. Darej,³⁹ U. Goerlach³⁹, C. Grimault,³⁹ A.-C. Le Bihan³⁹, P. Van Hove³⁹, S. Beauceron⁴⁰, B. Blancon⁴⁰, G. Boudoul⁴⁰, A. Carle,⁴⁰ N. Chanon⁴⁰,

- J. Choi⁴⁰ D. Contardo⁴⁰ P. Depasse⁴⁰ C. Dozen^{40,r} H. El Mamouni⁴⁰ J. Fay⁴⁰ S. Gascon⁴⁰ M. Gouzevitch⁴⁰
 G. Grenier⁴⁰ B. Ille⁴⁰ I. B. Laktineh⁴⁰ M. Lethuillier⁴⁰ L. Mirabito⁴⁰ S. Perries⁴⁰ L. Torterot⁴⁰
 M. Vander Donckt⁴⁰ P. Verdier⁴⁰ S. Viret⁴⁰ D. Chokheli⁴¹ I. Lomidze⁴¹ Z. Tsamalaidze^{41,k} V. Botta⁴²
 L. Feld⁴² K. Klein⁴² M. Lipinski⁴² D. Meuser⁴² A. Pauls⁴² N. Röwert⁴² M. Teroerde⁴² S. Diekmann⁴³
 A. Dodonova⁴³ N. Eich⁴³ D. Eliseev⁴³ M. Erdmann⁴³ P. Fackeldey⁴³ D. Fasanella⁴³ B. Fischer⁴³
 T. Hebbeker⁴³ K. Hoepfner⁴³ F. Ivone⁴³ M. y. Lee⁴³ L. Mastrolorenzo⁴³ M. Merschmeyer⁴³ A. Meyer⁴³
 S. Mondal⁴³ S. Mukherjee⁴³ D. Noll⁴³ A. Novak⁴³ F. Nowotny⁴³ A. Pozdnyakov⁴³ Y. Rath⁴³ W. Redjeb⁴³
 F. Rehm⁴³ H. Reithler⁴³ A. Schmidt⁴³ S. C. Schuler⁴³ A. Sharma⁴³ A. Stein⁴³ F. Torres Da Silva De Araujo^{43,s}
 L. Vigilante⁴³ S. Wiedenbeck⁴³ S. Zaleski⁴³ C. Dziwok⁴⁴ G. Flügge⁴⁴ W. Haj Ahmad^{44,t} O. Hlushchenko⁴⁴
 T. Kress⁴⁴ A. Nowack⁴⁴ O. Pooth⁴⁴ A. Stahl⁴⁴ T. Ziemons⁴⁴ A. Zott⁴⁴ H. Aarup Petersen⁴⁵
 M. Aldaya Martin⁴⁵ J. Alimena⁴⁵ P. Asmuss⁴⁵ S. Baxter⁴⁵ M. Bayatmakou⁴⁵ H. Becerril Gonzalez⁴⁵
 O. Behnke⁴⁵ S. Bhattacharya⁴⁵ F. Blekman^{45,u} K. Borras^{45,v} D. Brunner⁴⁵ A. Campbell⁴⁵ A. Cardini⁴⁵
 C. Cheng⁴⁵ F. Colombina⁴⁵ S. Consuegra Rodríguez⁴⁵ G. Correia Silva⁴⁵ M. De Silva⁴⁵ G. Eckerlin⁴⁵
 D. Eckstein⁴⁵ L. I. Estevez Banos⁴⁵ O. Filatov⁴⁵ E. Gallo^{45,u} A. Geiser⁴⁵ A. Giraldi⁴⁵ G. Greau⁴⁵
 A. Grohsjean⁴⁵ V. Guglielmi⁴⁵ M. Guthoff⁴⁵ A. Jafari^{45,w} N. Z. Jomhari⁴⁵ B. Kaech⁴⁵ M. Kasemann⁴⁵
 H. Kaveh⁴⁵ C. Kleinwort⁴⁵ R. Kogler⁴⁵ M. Komm⁴⁵ D. Krücker⁴⁵ W. Lange⁴⁵ D. Leyva Pernia⁴⁵
 K. Lipka^{45,x} W. Lohmann^{45,y} R. Mankel⁴⁵ I.-A. Melzer-Pellmann⁴⁵ M. Mendizabal Morentin⁴⁵ J. Metwally⁴⁵
 A. B. Meyer⁴⁵ G. Milella⁴⁵ M. Mormile⁴⁵ A. Mussgiller⁴⁵ A. Nürnberg⁴⁵ Y. Otarid⁴⁵ D. Pérez Adán⁴⁵
 E. Ranken⁴⁵ A. Raspereza⁴⁵ B. Ribeiro Lopes⁴⁵ J. Rübenach⁴⁵ A. Saggio⁴⁵ M. Savitsky⁴⁵ M. Scham^{45,v,z}
 V. Scheurer⁴⁵ S. Schnake^{45,v} P. Schütze⁴⁵ C. Schwanenberger^{45,u} M. Shchedrolosiev⁴⁵ R. E. Sosa Ricardo⁴⁵
 D. Stafford⁴⁵ N. Tonon^{45,o} M. Van De Klundert⁴⁵ F. Vazzoler⁴⁵ A. Velyka⁴⁵ A. Ventura Barroso⁴⁵ R. Walsh⁴⁵
 D. Walter⁴⁵ Q. Wang⁴⁵ Y. Wen⁴⁵ K. Wichmann⁴⁵ L. Wiens^{45,v} C. Wissing⁴⁵ S. Wuchterl⁴⁵ Y. Yang⁴⁵
 A. Zimermann Castro Santos⁴⁵ A. Albrecht⁴⁶ S. Albrecht⁴⁶ M. Antonello⁴⁶ S. Bein⁴⁶ L. Benato⁴⁶
 M. Bonanomi⁴⁶ P. Connor⁴⁶ K. De Leo⁴⁶ M. Eich⁴⁶ K. El Morabit⁴⁶ F. Feindt⁴⁶ A. Fröhlich⁴⁶ C. Garbers⁴⁶
 E. Garutti⁴⁶ M. Hajheidari⁴⁶ J. Haller⁴⁶ A. Hinzmann⁴⁶ H. R. Jabusch⁴⁶ G. Kasieczka⁴⁶ P. Keicher⁴⁶
 R. Klanner⁴⁶ W. Korcari⁴⁶ T. Kramer⁴⁶ V. Kutzner⁴⁶ F. Labe⁴⁶ J. Lange⁴⁶ A. Lobanov⁴⁶ C. Matthies⁴⁶
 A. Mehta⁴⁶ L. Moureaux⁴⁶ M. Mrowietz⁴⁶ A. Nigamova⁴⁶ Y. Nissan⁴⁶ A. Paasch⁴⁶ K. J. Pena Rodriguez⁴⁶
 T. Quadfasel⁴⁶ M. Rieger⁴⁶ D. Savoie⁴⁶ J. Schindler⁴⁶ P. Schleper⁴⁶ M. Schröder⁴⁶ J. Schwandt⁴⁶
 M. Sommerhalder⁴⁶ H. Stadie⁴⁶ G. Steinbrück⁴⁶ A. Tews⁴⁶ M. Wolf⁴⁶ S. Brommer⁴⁷ M. Burkart⁴⁷ E. Butz⁴⁷
 T. Chwalek⁴⁷ A. Dierlamm⁴⁷ A. Droll⁴⁷ N. Faltermann⁴⁷ M. Giffels⁴⁷ J. O. Gosewisch⁴⁷ A. Gottmann⁴⁷
 F. Hartmann^{47,aa} M. Horzela⁴⁷ U. Husemann⁴⁷ M. Klute⁴⁷ R. Koppenhöfer⁴⁷ M. Link⁴⁷ A. Lintuluoto⁴⁷
 S. Maier⁴⁷ S. Mitra⁴⁷ Th. Müller⁴⁷ M. Neukum⁴⁷ M. Oh⁴⁷ G. Quast⁴⁷ K. Rabbertz⁴⁷ I. Shvetsov⁴⁷
 H. J. Simonis⁴⁷ N. Trevisani⁴⁷ R. Ulrich⁴⁷ J. van der Linden⁴⁷ R. F. Von Cube⁴⁷ M. Wassmer⁴⁷ S. Wieland⁴⁷
 R. Wolf⁴⁷ S. Wozniewski⁴⁷ S. Wunsch⁴⁷ X. Zuo⁴⁷ G. Anagnostou⁴⁸ P. Assiouras⁴⁸ G. Daskalakis⁴⁸
 A. Kyriakis⁴⁸ A. Stakia⁴⁸ M. Diamantopoulou⁴⁹ D. Karasavvas⁴⁹ P. Kontaxakis⁴⁹ A. Manousakis-Katsikakis⁴⁹
 A. Panagiotou⁴⁹ I. Papavergou⁴⁹ N. Saoulidou⁴⁹ K. Theofilatos⁴⁹ E. Tziaferi⁴⁹ K. Vellidis⁴⁹ I. Zisopoulos⁴⁹
 G. Bakas⁵⁰ T. Chatzistavrou⁵⁰ G. Karapostoli⁵⁰ K. Kousouris⁵⁰ I. Papakrivopoulos⁵⁰ G. Tsipolitis⁵⁰
 A. Zacharopoulou⁵⁰ K. Adamidis⁵¹ I. Bestintzanos⁵¹ I. Evangelou⁵¹ C. Foudas⁵¹ P. Gianneios⁵¹ C. Kamtsikis⁵¹
 P. Katsoulis⁵¹ P. Kokkas⁵¹ P. G. Kosmoglou Kioseoglou⁵¹ N. Manthos⁵¹ I. Papadopoulos⁵¹ J. Strologas⁵¹
 M. Csanád⁵² K. Farkas⁵² M. M. A. Gadallah⁵² B. Kórodi⁵² P. Major⁵² K. Mandal⁵² G. Pásztor⁵²
 A. J. Rádl^{52,ac} O. Surányi⁵² G. I. Veres⁵² M. Bartók^{53,ad} G. Bencze⁵³ C. Hajdu⁵³ D. Horvath^{53,ae,af}
 F. Sikler⁵³ V. Veszpremi⁵³ N. Beni⁵⁴ S. Czellar⁵⁴ J. Karancsi^{54,ad} J. Molnar⁵⁴ Z. Szillasi⁵⁴ D. Teyssier⁵⁴
 P. Raics⁵⁵ B. Ujvari^{55,ag} G. Zilizi⁵⁵ T. Csorgo^{56,ac} F. Nemes^{56,ac} T. Novak⁵⁶ J. Babbar⁵⁷ S. Bansal⁵⁷
 S. B. Beri⁵⁷ V. Bhatnagar⁵⁷ G. Chaudhary⁵⁷ S. Chauhan⁵⁷ N. Dhingra^{57,ah} R. Gupta⁵⁷ A. Kaur⁵⁷ A. Kaur⁵⁷
 H. Kaur⁵⁷ M. Kaur⁵⁷ S. Kumar⁵⁷ P. Kumari⁵⁷ M. Meena⁵⁷ K. Sandeep⁵⁷ T. Sheokand⁵⁷ J. B. Singh^{57,ai}
 A. Singla⁵⁷ A. Ahmed⁵⁸ A. Bhardwaj⁵⁸ A. Chhetri⁵⁸ B. C. Choudhary⁵⁸ A. Kumar⁵⁸ M. Naimuddin⁵⁸
 K. Ranjan⁵⁸ S. Saumya⁵⁸ S. Baradia⁵⁹ S. Barman^{59,aj} S. Bhattacharya⁵⁹ D. Bhowmik⁵⁹ S. Dutta⁵⁹ S. Dutta⁵⁹
 B. Gomber^{59,ak} M. Maity^{59,aj} P. Palit⁵⁹ G. Saha⁵⁹ B. Sahu⁵⁹ S. Sarkar⁵⁹ P. K. Behera⁶⁰ S. C. Behera⁶⁰
 S. Chatterjee⁶⁰ P. Kalbhor⁶⁰ J. R. Komaragiri^{60,al} D. Kumar^{60,al} A. Muhammad⁶⁰ L. Panwar^{60,al}
 R. Pradhan⁶⁰ P. R. Pujahari⁶⁰ N. R. Saha⁶⁰ A. Sharma⁶⁰ A. K. Sikdar⁶⁰ S. Verma⁶⁰ K. Naskar^{61,am} T. Aziz⁶²
 I. Das⁶² S. Dugad⁶² M. Kumar⁶² G. B. Mohanty⁶² P. Suryadevara⁶² S. Banerjee⁶³ M. Guchait⁶³ S. Karmakar⁶³
 S. Kumar⁶³ G. Majumder⁶³ K. Mazumdar⁶³ S. Mukherjee⁶³ A. Thachayath⁶³ S. Bahinipati^{64,an} A. K. Das⁶⁴
 C. Kar⁶⁴ P. Mal⁶⁴ T. Mishra⁶⁴ V. K. Muraleedharan Nair Bindhu^{64,ao} A. Nayak^{64,ao} P. Saha⁶⁴ S. K. Swain⁶⁴
 D. Vats^{64,ao} A. Alpana⁶⁵ S. Dube⁶⁵ B. Kansal⁶⁵ A. Laha⁶⁵ S. Pandey⁶⁵ A. Rastogi⁶⁵ S. Sharma⁶⁵
 H. Bakhshiansohi^{66,ap,ap} E. Khazaie^{66,ap} M. Zeinali^{66,ar} S. Chenarani^{67,as} S. M. Etesami⁶⁷ M. Khakzad⁶⁷
 M. Mohammadi Najafabadi⁶⁷ M. Grunewald⁶⁸ M. Abbrescia^{69a,69b} R. Aly^{69a,69b,at} C. Aruta^{69a,69b} A. Colaleo^{69a}
 D. Creanza^{69a,69c} L. Cristella^{69a,69b} N. De Filippis^{69a,69c} M. De Palma^{69a,69b} A. Di Florio^{69a,69b}
 W. Elmetenawee^{69a,69b} F. Errico^{69a,69b} L. Fiore^{69a} G. Iaselli^{69a,69c} G. Maggi^{69a} M. Maggi^{69a}

- I. Margjeka ^{69a,69b} V. Mastrapasqua ^{69a,69b} S. My ^{69a,69b} S. Nuzzo ^{69a,69b} A. Pellecchia ^{69a,69b} A. Pompili ^{69a,69b}
G. Pugliese ^{69a,69c} R. Radogna ^{69a} D. Ramos ^{69a} A. Ranieri ^{69a} G. Selvaggi ^{69a,69b} L. Silvestris ^{69a}
F. M. Simone ^{69a,69b} Ü. Sözbilir ^{69a} A. Stamerra ^{69a} R. Venditti ^{69a} P. Verwilligen ^{69a} G. Abbiendi ^{70a}
- C. Battilana ^{70a,70b} D. Bonacorsi ^{70a,70b} L. Borgonovi ^{70a} L. Brigliadori ^{70a} R. Campanini ^{70a,70b} P. Capiluppi ^{70a,70b}
A. Castro ^{70a,70b} F. R. Cavallo ^{70a} M. Cuffiani ^{70a} G. M. Dallavalle ^{70a} T. Diotalevi ^{70a,70b} F. Fabbri ^{70a}
A. Fanfani ^{70a,70b} P. Giacomelli ^{70a} L. Giommi ^{70a,70b} C. Grandi ^{70a} L. Guiducci ^{70a,70b} S. Lo Meo ^{70a,au}
L. Lunerti ^{70a,70b} S. Marcellini ^{70a} G. Masetti ^{70a} F. L. Navarria ^{70a,70b} A. Perrotta ^{70a} F. Primavera ^{70a,70b}
A. M. Rossi ^{70a,70b} T. Rovelli ^{70a,70b} G. P. Siroli ^{70a,70b} S. Costa ^{71a,71b,av} A. Di Mattia ^{71a} R. Potenza ^{71a,71b}
A. Tricomi ^{71a,71b,av} C. Tuve ^{71a,71b} G. Barbagli ^{72a} G. Bardelli ^{72a,72b} B. Camaiani ^{72a,72b} A. Cassese ^{72a}
R. Ceccarelli ^{72a,72b} V. Ciulli ^{72a,72b} C. Civinini ^{72a} R. D'Alessandro ^{72a,72b} E. Focardi ^{72a,72b} G. Latino ^{72a,72b}
P. Lenzi ^{72a,72b} M. Lizzo ^{72a,72b} M. Meschini ^{72a} S. Paoletti ^{72a} G. Sguazzoni ^{72a} L. Viliani ^{72a} L. Benussi ⁷³
S. Bianco ⁷³ S. Meola ^{73,aw} D. Piccolo ⁷³ M. Bozzo ^{74a,74b} P. Chatagnon ^{74a} F. Ferro ^{74a} E. Robutti ^{74a}
S. Tosi ^{74a,74b} A. Benaglia ^{75a} G. Boldrini ^{75a} F. Brivio ^{75a,75b} F. Cetorelli ^{75a,75b} F. De Guio ^{75a,75b}
M. E. Dinardo ^{75a,75b} P. Dini ^{75a} S. Gennai ^{75a} A. Ghezzi ^{75a,75b} P. Govoni ^{75a,75b} L. Guzzi ^{75a,75b}
M. T. Lucchini ^{75a,75b} M. Malberti ^{75a} S. Malvezzi ^{75a} A. Massironi ^{75a} D. Menasce ^{75a} L. Moroni ^{75a}
M. Paganoni ^{75a,75b} D. Pedrini ^{75a} B. S. Pinolini ^{75a} S. Ragazzi ^{75a,75b} N. Redaelli ^{75a} T. Tabarelli de Fatis ^{75a,75b}
D. Zuolo ^{75a,75b} S. Buontempo ^{76a} A. Cagnotta ^{76a,76b,76c,76d} F. Carnevali ^{76a,76b} N. Cavallo ^{76a,76c} A. De Iorio ^{76a,76b}
F. Fabozzi ^{76a,76c} A. O. M. Iorio ^{76a,76b} L. Lista ^{76a,76b,ax} P. Paolucci ^{76a,aa} B. Rossi ^{76a} C. Sciacca ^{76a,76b}
P. Azzi ^{77a} N. Bacchetta ^{77a,ay} D. Bisello ^{77a,77b,77c} P. Bortignon ^{77a} A. Bragagnolo ^{77a,77b} P. Checchia ^{77a}
T. Dorigo ^{77a} F. Gasparini ^{77a,77b} U. Gasparini ^{77a,77b} G. Grossi ^{77a} L. Layer ^{77a,az} E. Lusiani ^{77a} M. Margoni ^{77a,77b}
A. T. Meneguzzo ^{77a,77b} M. Michelotto ^{77a} J. Pazzini ^{77a,77b} P. Ronchese ^{77a,77b} R. Rossin ^{77a,77b} F. Simonetto ^{77a,77b}
G. Strong ^{77a} M. Tosi ^{77a,77b} H. Yarar ^{77a,77b} M. Zanetti ^{77a,77b} P. Zotto ^{77a,77b} A. Zucchetta ^{77a,77b} G. Zumerle ^{77a,77b}
S. Abu Zeid ^{78a,ba} C. Aimè ^{78a,78b} A. Braghieri ^{78a} S. Calzaferri ^{78a,78b} D. Fiorina ^{78a,78b} P. Montagna ^{78a,78b}
V. Re ^{78a} C. Riccardi ^{78a,78b} P. Salvini ^{78a} I. Vai ^{78a,78b} P. Vitulo ^{78a,78b} P. Asenov ^{79a,bb} G. M. Bilei ^{79a}
D. Ciangottini ^{79a,79b} L. Fanò ^{79a,79b} M. Magherini ^{79a,79b} G. Mantovani ^{79a,79b} V. Mariani ^{79a,79b} M. Menichelli ^{79a}
F. Moscatelli ^{79a,bb} A. Piccinelli ^{79a,79b} M. Presilla ^{79a,79b} A. Rossi ^{79a,79b} A. Santoccchia ^{79a,79b} D. Spiga ^{79a}
T. Tedeschi ^{79a,79b} P. Azzurri ^{80a} G. Bagliesi ^{80a} V. Bertacchi ^{80a,80c} R. Bhattacharya ^{80a} L. Bianchini ^{80a,80b}
T. Boccali ^{80a} E. Bossini ^{80a,80b} D. Bruschini ^{80a,80c} R. Castaldi ^{80a} M. A. Ciocci ^{80a,80b} V. D'Amante ^{80a,80d}
R. Dell'Orso ^{80a} S. Donato ^{80a} A. Giassi ^{80a} F. Ligabue ^{80a,80c} D. Matos Figueiredo ^{80a} A. Messineo ^{80a,80b}
M. Musich ^{80a,80b} F. Palla ^{80a} S. Parolia ^{80a} G. Ramirez-Sanchez ^{80a,80c} A. Rizzi ^{80a,80b} G. Rolandi ^{80a,80c}
S. Roy Chowdhury ^{80a} T. Sarkar ^{80a} A. Scribano ^{80a} P. Spagnolo ^{80a} R. Tenchini ^{80a} G. Tonelli ^{80a,80b}
N. Turini ^{80a,80d} A. Venturi ^{80a} P. G. Verdini ^{80a} P. Barria ^{81a} M. Campana ^{81a,81b} F. Cavallari ^{81a} D. Del Re ^{81a,81b}
E. Di Marco ^{81a} M. Diemoz ^{81a} E. Longo ^{81a,81b} P. Meridiani ^{81a} G. Organtini ^{81a,81b} F. Pandolfi ^{81a}
R. Paramatti ^{81a,81b} C. Quaranta ^{81a,81b} S. Rahatlou ^{81a,81b} C. Rovelli ^{81a} F. Santanastasio ^{81a,81b} L. Soffi ^{81a}
R. Tramontano ^{81a,81b} N. Amapane ^{82a,82b} R. Arcidiacono ^{82a,82c} S. Argiro ^{82a,82b} M. Arneodo ^{82a,82c} N. Bartosik ^{82a}
R. Bellan ^{82a,82b} A. Bellora ^{82a,82b} C. Biino ^{82a} N. Cartiglia ^{82a} M. Costa ^{82a,82b} R. Covarelli ^{82a,82b} N. Demaria ^{82a}
M. Grippo ^{82a,82b} B. Kiani ^{82a,82b} F. Legger ^{82a} F. Luongo ^{82a,82b} C. Mariotti ^{82a} S. Maselli ^{82a} A. Mecca ^{82a,82b}
E. Migliore ^{82a,82b} M. Monteno ^{82a} R. Mulargia ^{82a} M. M. Obertino ^{82a,82b} G. Ortona ^{82a} L. Pacher ^{82a,82b}
N. Pastrone ^{82a,82b} M. Pelliccioni ^{82a} M. Ruspa ^{82a,82c} K. Shchelina ^{82a} F. Siviero ^{82a,82b} V. Sola ^{82a,82b}
A. Solano ^{82a,82b} D. Soldi ^{82a,82b} A. Staiano ^{82a} C. Tarricone ^{82a,82b} M. Tornago ^{82a,82b} D. Trocino ^{82a}
G. Umoret ^{82a,82b} A. Vagnerini ^{82a,82b} E. Vlasov ^{82a,82b} S. Belforte ^{83a} V. Candelise ^{83a,83b} M. Casarsa ^{83a}
F. Cossutti ^{83a} G. Della Ricca ^{83a,83b} G. Sorrentino ^{83a,83b} S. Dogra ⁸⁴ C. Huh ⁸⁴ B. Kim ⁸⁴ D. H. Kim ⁸⁴
G. N. Kim ⁸⁴ J. Kim ⁸⁴ J. Lee ⁸⁴ S. W. Lee ⁸⁴ C. S. Moon ⁸⁴ Y. D. Oh ⁸⁴ S. I. Pak ⁸⁴ M. S. Ryu ⁸⁴ S. Sekmen ⁸⁴
Y. C. Yang ⁸⁴ H. Kim ⁸⁵ D. H. Moon ⁸⁵ E. Asilar ⁸⁶ T. J. Kim ⁸⁶ J. Park ⁸⁶ S. Choi ⁸⁷ S. Han ⁸⁷ B. Hong ⁸⁷
K. Lee ⁸⁷ K. S. Lee ⁸⁷ J. Lim ⁸⁷ J. Park ⁸⁷ S. K. Park ⁸⁷ J. Yoo ⁸⁷ J. Goh ⁸⁸ H. S. Kim ⁸⁹ Y. Kim ⁸⁹ S. Lee ⁸⁹
J. Almond ⁹⁰ J. H. Bhyun ⁹⁰ J. Choi ⁹⁰ S. Jeon ⁹⁰ J. Kim ⁹⁰ J. S. Kim ⁹⁰ S. Ko ⁹⁰ H. Kwon ⁹⁰ H. Lee ⁹⁰ S. Lee ⁹⁰
B. H. Oh ⁹⁰ S. B. Oh ⁹⁰ H. Seo ⁹⁰ U. K. Yang ⁹⁰ I. Yoon ⁹⁰ W. Jang ⁹¹ D. Y. Kang ⁹¹ Y. Kang ⁹¹ D. Kim ⁹¹
S. Kim ⁹¹ B. Ko ⁹¹ J. S. H. Lee ⁹¹ Y. Lee ⁹¹ J. A. Merlin ⁹¹ I. C. Park ⁹¹ Y. Roh ⁹¹ D. Song ⁹¹ I. J. Watson ⁹¹
S. Yang ⁹¹ S. Ha ⁹² H. D. Yoo ⁹² M. Choi ⁹³ M. R. Kim ⁹³ H. Lee ⁹³ Y. Lee ⁹³ I. Yu ⁹³ T. Beyrouty ⁹⁴
Y. Maghrbi ⁹⁴ K. Dreimanis ⁹⁵ G. Pikurs ⁹⁵ A. Potrebko ⁹⁵ M. Seidel ⁹⁵ V. Veckalns ^{95,be} M. Ambrozias ⁹⁶
A. Carvalho Antunes De Oliveira ⁹⁶ A. Juodagalvis ⁹⁶ A. Rinkevicius ⁹⁶ G. Tamulaitis ⁹⁶ N. Bin Norjoharuddeen ⁹⁷
S. Y. Hoh ^{97,bd} I. Yusuff ^{97,bd} Z. Zolkapli ⁹⁷ J. F. Benitez ⁹⁸ A. Castaneda Hernandez ⁹⁸ H. A. Encinas Acosta ⁹⁸
L. G. Gallegos Maríñez ⁹⁸ M. León Coello ⁹⁸ J. A. Murillo Quijada ⁹⁸ A. Sehrawat ⁹⁸ L. Valencia Palomo ⁹⁸
G. Ayala ⁹⁹ H. Castilla-Valdez ⁹⁹ I. Heredia-De La Cruz ^{99,be} R. Lopez-Fernandez ⁹⁹ C. A. Mondragon Herrera ⁹⁹
D. A. Perez Navarro ⁹⁹ A. Sánchez Hernández ⁹⁹ C. Oropeza Barrera ¹⁰⁰ F. Vazquez Valencia ¹⁰⁰ I. Pedraza ¹⁰¹
H. A. Salazar Ibarguen ¹⁰¹ C. Uribe Estrada ¹⁰¹ I. Bubanja ¹⁰² J. Mijuskovic ^{102,bf} N. Raicevic ¹⁰² A. Ahmad ¹⁰³
M. I. Asghar ¹⁰³ A. Awais ¹⁰³ M. I. M. Awan ¹⁰³ M. Gul ¹⁰³ H. R. Hoorani ¹⁰³ W. A. Khan ¹⁰³ V. Avati ¹⁰⁴
L. Grzanka ¹⁰⁴ M. Malawski ¹⁰⁴ H. Bialkowska ¹⁰⁵ M. Bluj ¹⁰⁵ B. Boimska ¹⁰⁵ M. Górski ¹⁰⁵ M. Kazana ¹⁰⁵

- M. Szleper ¹⁰⁵, P. Zalewski ¹⁰⁵, K. Bunkowski ¹⁰⁶, K. Doroba ¹⁰⁶, A. Kalinowski ¹⁰⁶, M. Konecki ¹⁰⁶, J. Krolikowski ¹⁰⁶, M. Araujo ¹⁰⁷, P. Bargassa ¹⁰⁷, D. Bastos ¹⁰⁷, A. Boletti ¹⁰⁷, P. Faccioli ¹⁰⁷, M. Gallinaro ¹⁰⁷, J. Hollar ¹⁰⁷, N. Leonardo ¹⁰⁷, T. Niknejad ¹⁰⁷, M. Pisano ¹⁰⁷, J. Seixas ¹⁰⁷, J. Varela ¹⁰⁷, P. Adzic ^{108,bg}, M. Dordevic ¹⁰⁸, P. Milenovic ¹⁰⁸, J. Milosevic ¹⁰⁸, M. Aguilar-Benitez ¹⁰⁹, J. Alcaraz Maestre ¹⁰⁹, M. Barrio Luna, ¹⁰⁹ Cristina F. Bedoya ¹⁰⁹, M. Cepeda ¹⁰⁹, M. Cerrada ¹⁰⁹, N. Colino ¹⁰⁹, B. De La Cruz ¹⁰⁹, A. Delgado Peris ¹⁰⁹, D. Fernández Del Val ¹⁰⁹, J. P. Fernández Ramos ¹⁰⁹, J. Flix ¹⁰⁹, M. C. Fouz ¹⁰⁹, O. Gonzalez Lopez ¹⁰⁹, S. Goy Lopez ¹⁰⁹, J. M. Hernandez ¹⁰⁹, M. I. Josa ¹⁰⁹, J. León Holgado ¹⁰⁹, D. Moran ¹⁰⁹, C. Perez Dengra ¹⁰⁹, A. Pérez-Calero Yzquierdo ¹⁰⁹, J. Puerta Pelayo ¹⁰⁹, I. Redondo ¹⁰⁹, D. D. Redondo Ferrero ¹⁰⁹, L. Romero, ¹⁰⁹ S. Sánchez Navas ¹⁰⁹, J. Sastre ¹⁰⁹, L. Urda Gómez ¹⁰⁹, J. Vazquez Escobar ¹⁰⁹, C. Willmott, ¹⁰⁹ J. F. de Trocóniz ¹¹⁰, B. Alvarez Gonzalez ¹¹¹, J. Cuevas ¹¹¹, J. Fernandez Menendez ¹¹¹, S. Folgueras ¹¹¹, I. Gonzalez Caballero ¹¹¹, J. R. González Fernández ¹¹¹, E. Palencia Cortezon ¹¹¹, C. Ramón Álvarez ¹¹¹, V. Rodríguez Bouza ¹¹¹, A. Soto Rodríguez ¹¹¹, A. Trapote ¹¹¹, C. Vico Villalba ¹¹¹, J. A. Brochero Cifuentes ¹¹², I. J. Cabrillo ¹¹², A. Calderon ¹¹², J. Duarte Campderros ¹¹², M. Fernandez ¹¹², C. Fernandez Madrazo ¹¹², A. García Alonso, ¹¹² G. Gomez ¹¹², C. Lasosa Garcia ¹¹², C. Martinez Rivero ¹¹², P. Martinez Ruiz del Arbol ¹¹², F. Matorras ¹¹², P. Matorras Cuevas ¹¹², J. Piedra Gomez ¹¹², C. Prieels, ¹¹² L. Scodellaro ¹¹², I. Vila ¹¹², J. M. Vizan Garcia ¹¹², M. K. Jayananda ¹¹³, B. Kailasapathy ^{113,bh}, D. U. J. Sonnadar ¹¹³, D. D. C. Wickramarathna ¹¹³, W. G. D. Dharmaratna ¹¹⁴, K. Liyanage ¹¹⁴, N. Perera ¹¹⁴, N. Wickramage ¹¹⁴, D. Abbaneo ¹¹⁵, E. Auffray ¹¹⁵, G. Auzinger ¹¹⁵, J. Baechler, ¹¹⁵ P. Baillon, ^{115,o} D. Barney ¹¹⁵, J. Bendavid ¹¹⁵, A. Bermúdez Martínez ¹¹⁵, M. Bianco ¹¹⁵, B. Bilin ¹¹⁵, A. A. Bin Anuar ¹¹⁵, A. Bocci ¹¹⁵, E. Brondolin ¹¹⁵, C. Caillol ¹¹⁵, T. Camporesi ¹¹⁵, G. Cerminara ¹¹⁵, N. Chernyavskaya ¹¹⁵, S. S. Chhibra ¹¹⁵, S. Choudhury, ¹¹⁵ M. Cipriani ¹¹⁵, D. d'Enterria ¹¹⁵, A. Dabrowski ¹¹⁵, A. David ¹¹⁵, A. De Roeck ¹¹⁵, M. M. Defranchis ¹¹⁵, M. Deile ¹¹⁵, M. Dobson ¹¹⁵, M. Dünser ¹¹⁵, N. Dupont, ¹¹⁵ F. Fallavollita, ^{115,bi} A. Florent ¹¹⁵, L. Forthomme ¹¹⁵, G. Franzoni ¹¹⁵, W. Funk ¹¹⁵, S. Ghosh ¹¹⁵, S. Giani, ¹¹⁵, D. Gigi ¹¹⁵, K. Gill ¹¹⁵, F. Glege ¹¹⁵, L. Gouskos ¹¹⁵, E. Govorkova ¹¹⁵, M. Haranko ¹¹⁵, J. Hegeman ¹¹⁵, V. Innocente ¹¹⁵, T. James ¹¹⁵, P. Janot ¹¹⁵, J. Kaspar ¹¹⁵, J. Kieseler ¹¹⁵, N. Kratochwil ¹¹⁵, S. Laurila ¹¹⁵, P. Lecoq ¹¹⁵, E. Leutgeb ¹¹⁵, C. Lourenço ¹¹⁵, B. Maier ¹¹⁵, L. Malgeri ¹¹⁵, M. Mannelli ¹¹⁵, A. C. Marini ¹¹⁵, F. Meijers ¹¹⁵, S. Mersi ¹¹⁵, E. Meschi ¹¹⁵, F. Moortgat ¹¹⁵, M. Mulders ¹¹⁵, S. Orfanelli, ¹¹⁵ L. Orsini, ¹¹⁵ F. Pantaleo ¹¹⁵, E. Perez, ¹¹⁵ M. Peruzzi ¹¹⁵, A. Petrilli ¹¹⁵, G. Petrucciani ¹¹⁵, A. Pfeiffer ¹¹⁵, M. Pierini ¹¹⁵, D. Piparo ¹¹⁵, M. Pitt ¹¹⁵, H. Qu ¹¹⁵, T. Quast, ¹¹⁵ D. Rabady ¹¹⁵, A. Racz, ¹¹⁵ G. Reales Gutierrez, ¹¹⁵ M. Rovere ¹¹⁵, H. Sakulin ¹¹⁵, J. Salfeld-Nebgen ¹¹⁵, S. Scarfi ¹¹⁵, M. Selvaggi ¹¹⁵, A. Sharma ¹¹⁵, P. Silva ¹¹⁵, P. Sphicas ^{115,bj}, A. G. Stahl Leiton ¹¹⁵, S. Summers ¹¹⁵, K. Tatar ¹¹⁵, D. Treille ¹¹⁵, P. Tropea ¹¹⁵, A. Tsirou, ¹¹⁵ J. Wanczyk ^{115,bk}, K. A. Wozniak ¹¹⁵, W. D. Zeuner, ¹¹⁵ L. Caminada ^{116,bl}, A. Ebrahimi ¹¹⁶, W. Erdmann ¹¹⁶, R. Horisberger ¹¹⁶, Q. Ingram ¹¹⁶, H. C. Kaestli ¹¹⁶, D. Kotlinski ¹¹⁶, C. Lange ¹¹⁶, M. Missiroli ^{116,bl}, L. Noehte ^{116,bl}, T. Rohe ¹¹⁶, T. K. Arrestad ¹¹⁷, K. Androsov ^{117,bk}, M. Backhaus ¹¹⁷, A. Calandri ¹¹⁷, K. Datta ¹¹⁷, A. De Cosa ¹¹⁷, G. Dissertori ¹¹⁷, M. Dittmar, ¹¹⁷ M. Donegà ¹¹⁷, F. Eble ¹¹⁷, M. Galli ¹¹⁷, K. Gedia ¹¹⁷, F. Glessgen ¹¹⁷, T. A. Gómez Espinosa ¹¹⁷, C. Grab ¹¹⁷, D. Hits ¹¹⁷, W. Lustermann ¹¹⁷, A.-M. Lyon ¹¹⁷, R. A. Manzoni ¹¹⁷, L. Marchese ¹¹⁷, C. Martin Perez ¹¹⁷, A. Mascellani ^{117,bk}, F. Nessi-Tedaldi ¹¹⁷, J. Niedziela ¹¹⁷, F. Pauss ¹¹⁷, V. Perovic ¹¹⁷, S. Pigazzini ¹¹⁷, M. G. Ratti ¹¹⁷, M. Reichmann ¹¹⁷, C. Reissel ¹¹⁷, T. Reitenspiess ¹¹⁷, B. Ristic ¹¹⁷, F. Riti ¹¹⁷, D. Ruini, ¹¹⁷ D. A. Sanz Becerra ¹¹⁷, R. Seidita ¹¹⁷, J. Steggemann ^{117,bk}, D. Valsecchi ¹¹⁷, R. Wallny ¹¹⁷, C. Amsler ^{118,bm}, P. Bärtschi ¹¹⁸, C. Botta ¹¹⁸, D. Brzhechko, ¹¹⁸ M. F. Canelli ¹¹⁸, K. Cormier ¹¹⁸, A. De Wit ¹¹⁸, R. Del Burgo, ¹¹⁸ J. K. Heikkilä ¹¹⁸, M. Huwiler ¹¹⁸, W. Jin ¹¹⁸, A. Jofrehei ¹¹⁸, B. Kilminster ¹¹⁸, S. Leontsinis ¹¹⁸, S. P. Liechti ¹¹⁸, A. Macchiolo ¹¹⁸, P. Meiring ¹¹⁸, V. M. Mikuni ¹¹⁸, U. Molinatti ¹¹⁸, I. Neutelings ¹¹⁸, A. Reimers ¹¹⁸, P. Robmann, ¹¹⁸ S. Sanchez Cruz ¹¹⁸, K. Schweiger ¹¹⁸, M. Singer ¹¹⁸, Y. Takahashi ¹¹⁸, C. Adloff, ^{119,bl} C. M. Kuo, ¹¹⁹, W. Lin, ¹¹⁹, P. K. Rout ¹¹⁹, P. C. Tiwari ^{119,al}, S. S. Yu ¹¹⁹, L. Ceard, ¹²⁰, Y. Chao ¹²⁰, K. F. Chen ¹²⁰, P. s. Chen, ¹²⁰, H. Cheng ¹²⁰, W.-S. Hou ¹²⁰, R. Khurana, ¹²⁰, G. Kole ¹²⁰, Y. y. Li ¹²⁰, R.-S. Lu ¹²⁰, E. Paganis ¹²⁰, A. Psallidas, ¹²⁰, A. Steen ¹²⁰, H. y. Wu, ¹²⁰, E. Yazgan ¹²⁰, C. Asawatangtrakuldee ¹²¹, N. Sriamanobhas ¹²¹, V. Wachirapusanand ¹²¹, D. Agyel ¹²², F. Boran ¹²², Z. S. Demiroglu ¹²², F. Dolek ¹²², I. Dumanoglu ^{122,bo}, E. Eskut ¹²², Y. Guler ^{122,bl}, E. Gurpinar Guler ^{122,bl}, C. Isik ¹²², O. Kara, ¹²², A. Kayis Topaksu ¹²², U. Kiminsu ¹²², G. Onengut ¹²², K. Ozdemir ^{122,bq}, A. Polatoz ¹²², A. E. Simsek ¹²², B. Tali ^{122,br}, U. G. Tok ¹²², S. Turkcapar ¹²², E. Uslan ¹²², I. S. Zorbakir ¹²², G. Karapinar, ^{123,bs}, K. Ocalan ^{123,bs}, M. Yalvac ^{123,bs}, B. Akgun ¹²⁴, I. O. Atakisi ¹²⁴, E. Gülmез ¹²⁴, M. Kaya ^{124,bv}, O. Kaya ^{124,bw}, S. Tekten ^{124,bx}, A. Cakir ¹²⁵, K. Cankocak ^{125,bo}, Y. Komurcu ¹²⁵, S. Sen ^{125,by}, O. Aydilek ¹²⁶, S. Cerci ^{126,br}, B. Hacisahinoglu ¹²⁶, I. Hos ^{126,bz}, B. Isildak ^{126,ca}, B. Kaynak ¹²⁶, S. Ozkorucuklu ¹²⁶, C. Simsek ¹²⁶, D. Sunar Cerci ^{126,br}, B. Grynyov ¹²⁷, L. Levchuk ¹²⁸, D. Anthony ¹²⁹, J. J. Brooke ¹²⁹, A. Bundock ¹²⁹, E. Clement ¹²⁹, D. Cussans ¹²⁹, H. Flacher ¹²⁹, M. Glowacki, ¹²⁹, J. Goldstein ¹²⁹, H. F. Heath ¹²⁹, L. Kreczko ¹²⁹, B. Krikler ¹²⁹, S. Paramesvaran ¹²⁹, S. Seif El Nasr-Storey, ¹²⁹, V. J. Smith ¹²⁹, N. Stylianou ^{129,cb}, K. Walkingshaw Pass, ¹²⁹, R. White ¹²⁹, A. H. Ball, ¹³⁰, K. W. Bell ¹³⁰, A. Belyaev ^{130,cc}, C. Brew ¹³⁰, R. M. Brown ¹³⁰, D. J. A. Cockerill ¹³⁰, C. Cooke ¹³⁰, K. V. Ellis, ¹³⁰, K. Harder ¹³⁰, S. Harper ¹³⁰, M.-L. Holmberg ^{130,cd}, Sh. Jain ¹³⁰, J. Linacre ¹³⁰, K. Manolopoulos, ¹³⁰, D. M. Newbold ¹³⁰, E. Olaiya, ¹³⁰, D. Petyt ¹³⁰, T. Reis ¹³⁰, G. Salvi ¹³⁰, T. Schuh, ¹³⁰, C. H. Shepherd-Themistocleous ¹³⁰, I. R. Tomalin ¹³⁰, T. Williams ¹³⁰

- R. Bainbridge¹³¹ P. Bloch¹³¹ S. Bonomally¹³¹ J. Borg¹³¹ C. E. Brown¹³¹ O. Buchmuller¹³¹ V. Cacchio¹³¹
 C. A. Carrillo Montoya¹³¹ V. Cepaitis¹³¹ G. S. Chahal^{131,ce} D. Colling¹³¹ J. S. Dancu¹³¹ P. Dauncey¹³¹
 G. Davies¹³¹ J. Davies¹³¹ M. Della Negra¹³¹ S. Fayer¹³¹
 G. Fedi¹³¹ G. Hall¹³¹ M. H. Hassanshahi¹³¹ A. Howard¹³¹ G. Iles¹³¹ J. Langford¹³¹ L. Lyons¹³¹
 A.-M. Magnan¹³¹ S. Malik¹³¹ A. Martelli¹³¹ M. Mieskolainen¹³¹ D. G. Monk¹³¹ J. Nash^{131,cf} M. Pesaresi¹³¹
 B. C. Radburn-Smith¹³¹ D. M. Raymond¹³¹ A. Richards¹³¹ A. Rose¹³¹ E. Scott¹³¹ C. Seez¹³¹ R. Shukla¹³¹
 A. Tapper¹³¹ K. Uchida¹³¹ G. P. Uttley¹³¹ L. H. Vage¹³¹ T. Virdee^{131,aa} M. Vojinovic¹³¹ N. Wardle¹³¹
 S. N. Webb¹³¹ D. Winterbottom¹³¹ K. Coldham¹³² J. E. Cole¹³² A. Khan¹³² P. Kyberd¹³² I. D. Reid¹³²
 S. Abdullin¹³³ A. Brinkerhoff¹³³ B. Caraway¹³³ J. Dittmann¹³³ K. Hatakeyama¹³³ A. R. Kanuganti¹³³
 B. McMaster¹³³ M. Saunders¹³³ S. Sawant¹³³ C. Sutantawibul¹³³ M. Toms¹³³ J. Wilson¹³³ R. Bartek¹³⁴
 A. Dominguez¹³⁴ C. Huerta Escamilla¹³⁴ R. Uniyal¹³⁴ A. M. Vargas Hernandez¹³⁴ R. Chudasama¹³⁵
 S. I. Cooper¹³⁵ D. Di Croce¹³⁵ S. V. Gleyzer¹³⁵ C. U. Perez¹³⁵ P. Rumerio^{135,cg} E. Usai¹³⁵ C. West¹³⁵
 A. Akpinar¹³⁶ A. Albert¹³⁶ D. Arcaro¹³⁶ C. Cosby¹³⁶ Z. Demiragli¹³⁶ C. Erice¹³⁶ E. Fontanesi¹³⁶
 D. Gastler¹³⁶ S. May¹³⁶ J. Rohlfs¹³⁶ K. Salyer¹³⁶ D. Sperka¹³⁶ D. Spitzbart¹³⁶ I. Suarez¹³⁶ A. Tsatsos¹³⁶
 S. Yuan¹³⁶ G. Benelli¹³⁷ X. Coubez^{137,v} D. Cutts¹³⁷ M. Hadley¹³⁷ U. Heintz¹³⁷ J. M. Hogan^{137,eh}
 T. Kwon¹³⁷ G. Landsberg¹³⁷ K. T. Lau¹³⁷ D. Li¹³⁷ J. Luo¹³⁷ M. Narain¹³⁷ N. Pervan¹³⁷ S. Sagir¹³⁷
 F. Simpson¹³⁷ W. Y. Wong¹³⁷ X. Yan¹³⁷ D. Yu¹³⁷ W. Zhang¹³⁷ S. Abbott¹³⁸ J. Bonilla¹³⁸ C. Brainerd¹³⁸
 R. Breedon¹³⁸ M. Calderon De La Barca Sanchez¹³⁸ M. Chertok¹³⁸ J. Conway¹³⁸ P. T. Cox¹³⁸ R. Erbacher¹³⁸
 G. Haza¹³⁸ F. Jensen¹³⁸ O. Kukral¹³⁸ G. Mocellin¹³⁸ M. Mulhearn¹³⁸ D. Pellett¹³⁸ B. Regnery¹³⁸ Y. Yao¹³⁸
 F. Zhang¹³⁸ M. Bachtis¹³⁹ R. Cousins¹³⁹ A. Datta¹³⁹ J. Hauser¹³⁹ M. Ignatenko¹³⁹ M. A. Iqbal¹³⁹
 T. Lam¹³⁹ E. Manca¹³⁹ W. A. Nash¹³⁹ D. Saltzberg¹³⁹ B. Stone¹³⁹ V. Valuev¹³⁹ R. Clare¹⁴⁰ J. W. Gary¹⁴⁰
 M. Gordon¹⁴⁰ G. Hanson¹⁴⁰ O. R. Long¹⁴⁰ N. Manganelli¹⁴⁰ W. Si¹⁴⁰ S. Wimpenny¹⁴⁰ J. G. Branson¹⁴¹
 S. Cittolin¹⁴¹ S. Cooperstein¹⁴¹ D. Diaz¹⁴¹ J. Duarte¹⁴¹ R. Gerosa¹⁴¹ L. Giannini¹⁴¹ J. Guiang¹⁴¹
 R. Kansal¹⁴¹ V. Krutelyov¹⁴¹ R. Lee¹⁴¹ J. Letts¹⁴¹ M. Masciovecchio¹⁴¹ F. Mokhtar¹⁴¹ M. Pieri¹⁴¹
 M. Quinnan¹⁴¹ B. V. Sathia Narayanan¹⁴¹ V. Sharma¹⁴¹ M. Tadel¹⁴¹ E. Vourliotis¹⁴¹ F. Würthwein¹⁴¹
 Y. Xiang¹⁴¹ A. Yagil¹⁴¹ C. Campagnari¹⁴² M. Citron¹⁴² G. Collura¹⁴² A. Dorsett¹⁴² J. Incandela¹⁴²
 M. Kilpatrick¹⁴² J. Kim¹⁴² A. J. Li¹⁴² P. Masterson¹⁴² H. Mei¹⁴² M. Oshiro¹⁴² J. Richman¹⁴² U. Sarica¹⁴²
 R. Schmitz¹⁴² F. Setti¹⁴² J. Sheplock¹⁴² P. Siddireddy¹⁴² D. Stuart¹⁴² S. Wang¹⁴² A. Bornheim¹⁴³ O. Cerri¹⁴³
 I. Dutta¹⁴³ A. Latorre¹⁴³ J. M. Lawhorn¹⁴³ J. Mao¹⁴³ H. B. Newman¹⁴³ T. Q. Nguyen¹⁴³ M. Spiropulu¹⁴³
 J. R. Vlimant¹⁴³ C. Wang¹⁴³ S. Xie¹⁴³ R. Y. Zhu¹⁴³ J. Alison¹⁴⁴ S. An¹⁴⁴ M. B. Andrews¹⁴⁴ P. Bryant¹⁴⁴
 V. Dutta¹⁴⁴ T. Ferguson¹⁴⁴ A. Harilal¹⁴⁴ C. Liu¹⁴⁴ T. Mudholkar¹⁴⁴ S. Murthy¹⁴⁴ M. Paulini¹⁴⁴
 A. Roberts¹⁴⁴ A. Sanchez¹⁴⁴ W. Terrill¹⁴⁴ J. P. Cumalat¹⁴⁵ W. T. Ford¹⁴⁵ A. Hassani¹⁴⁵ G. Karathanasis¹⁴⁵
 E. MacDonald¹⁴⁵ F. Marini¹⁴⁵ A. Perloff¹⁴⁵ C. Savard¹⁴⁵ N. Schonbeck¹⁴⁵ K. Stenson¹⁴⁵ K. A. Ulmer¹⁴⁵
 S. R. Wagner¹⁴⁵ N. Zipper¹⁴⁵ J. Alexander¹⁴⁶ S. Bright-Thonney¹⁴⁶ X. Chen¹⁴⁶ D. J. Cranshaw¹⁴⁶ J. Fan¹⁴⁶
 X. Fan¹⁴⁶ D. Gadkari¹⁴⁶ S. Hogan¹⁴⁶ J. Monroy¹⁴⁶ J. R. Patterson¹⁴⁶ J. Reichert¹⁴⁶ M. Reid¹⁴⁶ A. Ryd¹⁴⁶
 J. Thom¹⁴⁶ P. Wittich¹⁴⁶ R. Zou¹⁴⁶ M. Albrow¹⁴⁷ M. Alyari¹⁴⁷ G. Apollinari¹⁴⁷ A. Apresyan¹⁴⁷
 L. A. T. Bauerdtick¹⁴⁷ D. Berry¹⁴⁷ J. Berryhill¹⁴⁷ P. C. Bhat¹⁴⁷ K. Burkett¹⁴⁷ J. N. Butler¹⁴⁷ A. Canepa¹⁴⁷
 G. B. Cerati¹⁴⁷ H. W. K. Cheung¹⁴⁷ F. Chlebana¹⁴⁷ K. F. Di Petillo¹⁴⁷ J. Dickinson¹⁴⁷ V. D. Elvira¹⁴⁷
 Y. Feng¹⁴⁷ J. Freeman¹⁴⁷ A. Gandrakota¹⁴⁷ Z. Gecse¹⁴⁷ L. Gray¹⁴⁷ D. Green¹⁴⁷ S. Grünendahl¹⁴⁷
 D. Guerrero¹⁴⁷ O. Gutsche¹⁴⁷ R. M. Harris¹⁴⁷ R. Heller¹⁴⁷ T. C. Herwig¹⁴⁷ J. Hirschauer¹⁴⁷ L. Horyn¹⁴⁷
 B. Jayatilaka¹⁴⁷ S. Jindariani¹⁴⁷ M. Johnson¹⁴⁷ U. Joshi¹⁴⁷ T. Klijnsma¹⁴⁷ B. Klima¹⁴⁷ K. H. M. Kwok¹⁴⁷
 S. Lammel¹⁴⁷ D. Lincoln¹⁴⁷ R. Lipton¹⁴⁷ T. Liu¹⁴⁷ C. Madrid¹⁴⁷ K. Maeshima¹⁴⁷ C. Mantilla¹⁴⁷
 D. Mason¹⁴⁷ P. McBride¹⁴⁷ P. Merkel¹⁴⁷ S. Mrenna¹⁴⁷ S. Nahm¹⁴⁷ J. Ngadiuba¹⁴⁷ D. Noonan¹⁴⁷
 S. Norberg¹⁴⁷ V. Papadimitriou¹⁴⁷ N. Pastika¹⁴⁷ K. Pedro¹⁴⁷ C. Pena^{147,cj} F. Ravera¹⁴⁷ A. Reinsvold Hall^{147,ck}
 L. Ristori¹⁴⁷ E. Sexton-Kennedy¹⁴⁷ N. Smith¹⁴⁷ A. Soha¹⁴⁷ L. Spiegel¹⁴⁷ J. Strait¹⁴⁷ L. Taylor¹⁴⁷
 S. Tkaczyk¹⁴⁷ N. V. Tran¹⁴⁷ L. Uplegger¹⁴⁷ E. W. Vaandering¹⁴⁷ I. Zoi¹⁴⁷ P. Avery¹⁴⁸ D. Bourilkov¹⁴⁸
 L. Cadamuro¹⁴⁸ P. Chang¹⁴⁸ V. Cherepanov¹⁴⁸ R. D. Field¹⁴⁸ E. Koenig¹⁴⁸ M. Kolosova¹⁴⁸ J. Konigsberg¹⁴⁸
 A. Korytov¹⁴⁸ E. Kuznetsova^{148,cl} K. H. Lo¹⁴⁸ K. Matchev¹⁴⁸ N. Menendez¹⁴⁸ G. Mitselmakher¹⁴⁸
 A. Muthirakalayil Madhu¹⁴⁸ N. Rawal¹⁴⁸ D. Rosenzweig¹⁴⁸ S. Rosenzweig¹⁴⁸ K. Shi¹⁴⁸ J. Wang¹⁴⁸ Z. Wu¹⁴⁸
 T. Adams¹⁴⁹ A. Askew¹⁴⁹ N. Bower¹⁴⁹ R. Habibullah¹⁴⁹ V. Haghopian¹⁴⁹ T. Kolberg¹⁴⁹ G. Martinez¹⁴⁹
 H. Prosper¹⁴⁹ O. Viazlo¹⁴⁹ M. Wulansatiti¹⁴⁹ R. Yohay¹⁴⁹ J. Zhang¹⁴⁹ M. M. Baarmand¹⁵⁰ S. Butalla¹⁵⁰
 T. Elkafrawy^{150,ba} M. Hohlmann¹⁵⁰ R. Kumar Verma¹⁵⁰ M. Rahmani¹⁵⁰ F. Yumiceva¹⁵⁰ M. R. Adams¹⁵¹
 R. Cavanaugh¹⁵¹ S. Dittmer¹⁵¹ O. Evdokimov¹⁵¹ C. E. Gerber¹⁵¹ D. J. Hofman¹⁵¹ D. S. Lemos¹⁵¹
 A. H. Merrit¹⁵¹ C. Mills¹⁵¹ G. Oh¹⁵¹ T. Roy¹⁵¹ S. Rudrabhatla¹⁵¹ M. B. Tonjes¹⁵¹ N. Varelas¹⁵¹
 X. Wang¹⁵¹ Z. Ye¹⁵¹ J. Yoo¹⁵¹ M. Alhusseini¹⁵² K. Dilsiz^{152,cm} L. Emediato¹⁵² G. Karaman¹⁵²
 O. K. Köseyan¹⁵² J.-P. Merlo¹⁵² A. Mestvirishvili^{152,cn} J. Nachtman¹⁵² O. Neogi¹⁵² H. Ogul^{152,co} Y. Onel¹⁵²
 A. Penzo¹⁵² C. Snyder¹⁵² E. Tiras^{152,cp} O. Amram¹⁵³ B. Blumenfeld¹⁵³ L. Corcodilos¹⁵³ J. Davis¹⁵³
 A. V. Gritsan¹⁵³ S. Kyriacou¹⁵³ P. Maksimovic¹⁵³ J. Roskes¹⁵³ S. Sekhar¹⁵³ M. Swartz¹⁵³ T. Á. Vámi¹⁵³

- A. Abreu¹⁵⁴ L. F. Alcerro Alcerro¹⁵⁴ J. Anguiano¹⁵⁴ P. Baringer¹⁵⁴ A. Bean¹⁵⁴ Z. Flowers¹⁵⁴ J. King¹⁵⁴
 G. Krintiras¹⁵⁴ M. Lazarovits¹⁵⁴ C. Le Mahieu¹⁵⁴ C. Lindsey¹⁵⁴ J. Marquez¹⁵⁴ N. Minafra¹⁵⁴ M. Murray¹⁵⁴
 M. Nickel¹⁵⁴ C. Rogan¹⁵⁴ C. Royon¹⁵⁴ R. Salvatico¹⁵⁴ S. Sanders¹⁵⁴ C. Smith¹⁵⁴ Q. Wang¹⁵⁴ G. Wilson¹⁵⁴
 B. Allmond¹⁵⁵ S. Duric¹⁵⁵ A. Ivanov¹⁵⁵ K. Kaadze¹⁵⁵ A. Kalogeropoulos¹⁵⁵ D. Kim¹⁵⁵ Y. Maravin¹⁵⁵
 T. Mitchell¹⁵⁵ A. Modak¹⁵⁵ K. Nam¹⁵⁵ D. Roy¹⁵⁵ F. Rebassoo¹⁵⁶ D. Wright¹⁵⁶ E. Adams¹⁵⁷ A. Baden¹⁵⁷
 O. Baron¹⁵⁷ A. Belloni¹⁵⁷ A. Bethani¹⁵⁷ S. C. Eno¹⁵⁷ N. J. Hadley¹⁵⁷ S. Jabeen¹⁵⁷ R. G. Kellogg¹⁵⁷
 T. Koeth¹⁵⁷ Y. Lai¹⁵⁷ S. Lascio¹⁵⁷ A. C. Mignerey¹⁵⁷ S. Nabili¹⁵⁷ C. Palmer¹⁵⁷ C. Papageorgakis¹⁵⁷
 L. Wang¹⁵⁷ K. Wong¹⁵⁷ W. Busza¹⁵⁸ I. A. Cali¹⁵⁸ Y. Chen¹⁵⁸ M. D'Alfonso¹⁵⁸ J. Eysermans¹⁵⁸ C. Freer¹⁵⁸
 G. Gomez-Ceballos¹⁵⁸ M. Goncharov¹⁵⁸ P. Harris¹⁵⁸ D. Kovalskyi¹⁵⁸ J. Krupa¹⁵⁸ Y.-J. Lee¹⁵⁸ K. Long¹⁵⁸
 C. Mironov¹⁵⁸ C. Paus¹⁵⁸ D. Rankin¹⁵⁸ C. Roland¹⁵⁸ G. Roland¹⁵⁸ Z. Shi¹⁵⁸ G. S. F. Stephans¹⁵⁸ J. Wang¹⁵⁸
 Z. Wang¹⁵⁸ B. Wyslouch¹⁵⁸ T. J. Yang¹⁵⁸ R. M. Chatterjee¹⁵⁹ B. Crossman¹⁵⁹ J. Hiltbrand¹⁵⁹ B. M. Joshi¹⁵⁹
 C. Kapsiak¹⁵⁹ M. Krohn¹⁵⁹ Y. Kubota¹⁵⁹ D. Mahon¹⁵⁹ J. Mans¹⁵⁹ M. Revering¹⁵⁹ R. Rusack¹⁵⁹
 R. Saradhy¹⁵⁹ N. Schroeder¹⁵⁹ N. Strobbe¹⁵⁹ M. A. Wadud¹⁵⁹ L. M. Cremaldi¹⁶⁰ K. Bloom¹⁶¹ M. Bryson¹⁶¹
 D. R. Claes¹⁶¹ C. Fangmeier¹⁶¹ L. Finco¹⁶¹ F. Golf¹⁶¹ C. Joo¹⁶¹ R. Kamalieddin¹⁶¹ I. Kravchenko¹⁶¹
 I. Reed¹⁶¹ J. E. Siado¹⁶¹ G. R. Snow¹⁶¹ W. Tabb¹⁶¹ A. Wightman¹⁶¹ F. Yan¹⁶¹ A. G. Zecchinelli¹⁶¹
 G. Agarwal¹⁶² H. Bandyopadhyay¹⁶² L. Hay¹⁶² I. Iashvili¹⁶² A. Kharchilava¹⁶² C. McLean¹⁶² M. Morris¹⁶²
 D. Nguyen¹⁶² J. Pekkanen¹⁶² S. Rappoccio¹⁶² A. Williams¹⁶² G. Alverson¹⁶³ E. Barberis¹⁶³ Y. Haddad¹⁶³
 Y. Han¹⁶³ A. Krishna¹⁶³ J. Li¹⁶³ J. Lidrych¹⁶³ G. Madigan¹⁶³ B. Marzocchi¹⁶³ D. M. Morse¹⁶³
 V. Nguyen¹⁶³ T. Orimoto¹⁶³ A. Parker¹⁶³ L. Skinnari¹⁶³ A. Tishelman-Charny¹⁶³ T. Wamorkar¹⁶³ B. Wang¹⁶³
 A. Wisecarver¹⁶³ D. Wood¹⁶³ S. Bhattacharya¹⁶⁴ J. Bueghly¹⁶⁴ Z. Chen¹⁶⁴ A. Gilbert¹⁶⁴ K. A. Hahn¹⁶⁴
 Y. Liu¹⁶⁴ N. Odell¹⁶⁴ M. H. Schmitt¹⁶⁴ M. Velasco¹⁶⁴ R. Band¹⁶⁵ R. Bucci¹⁶⁵ M. Cremonesi¹⁶⁵ A. Das¹⁶⁵
 R. Goldouzian¹⁶⁵ M. Hildreth¹⁶⁵ K. Hurtado Anampa¹⁶⁵ C. Jessop¹⁶⁵ K. Lannon¹⁶⁵ J. Lawrence¹⁶⁵
 N. Loukas¹⁶⁵ L. Lutton¹⁶⁵ J. Mariano¹⁶⁵ N. Marinelli¹⁶⁵ I. Mcalister¹⁶⁵ T. McCauley¹⁶⁵ C. Mcgrady¹⁶⁵
 K. Mohrman¹⁶⁵ C. Moore¹⁶⁵ Y. Musienko^{165,k} R. Ruchti¹⁶⁵ A. Townsend¹⁶⁵ M. Wayne¹⁶⁵ H. Yockey¹⁶⁵
 M. Zarucki¹⁶⁵ L. Zygal¹⁶⁵ B. Bylsma¹⁶⁶ M. Carrigan¹⁶⁶ L. S. Durkin¹⁶⁶ C. Hill¹⁶⁶ M. Joyce¹⁶⁶
 A. Lesauvage¹⁶⁶ M. Nunez Ornelas¹⁶⁶ K. Wei¹⁶⁶ B. L. Winer¹⁶⁶ B. R. Yates¹⁶⁶ F. M. Addesa¹⁶⁷ P. Das¹⁶⁷
 G. Dezoort¹⁶⁷ P. Elmer¹⁶⁷ A. Frankenthal¹⁶⁷ B. Greenberg¹⁶⁷ N. Haubrich¹⁶⁷ S. Higginbotham¹⁶⁷ G. Kopp¹⁶⁷
 S. Kwan¹⁶⁷ D. Lange¹⁶⁷ A. Loeliger¹⁶⁷ D. Marlow¹⁶⁷ I. Ojalvo¹⁶⁷ J. Olsen¹⁶⁷ D. Stickland¹⁶⁷ C. Tully¹⁶⁷
 S. Malik¹⁶⁸ A. S. Bakshi¹⁶⁹ V. E. Barnes¹⁶⁹ R. Chawla¹⁶⁹ S. Das¹⁶⁹ L. Gutay¹⁶⁹ M. Jones¹⁶⁹ A. W. Jung¹⁶⁹
 D. Kondratyev¹⁶⁹ A. M. Koshy¹⁶⁹ M. Liu¹⁶⁹ G. Negro¹⁶⁹ N. Neumeister¹⁶⁹ G. Paspalaki¹⁶⁹ S. Piperov¹⁶⁹
 A. Purohit¹⁶⁹ J. F. Schulte¹⁶⁹ M. Stojanovic^{169,p} J. Thieman¹⁶⁹ A. K. Virdi¹⁶⁹ F. Wang¹⁶⁹ R. Xiao¹⁶⁹
 W. Xie¹⁶⁹ J. Dolen¹⁷⁰ N. Parashar¹⁷⁰ D. Acosta¹⁷¹ A. Baty¹⁷¹ T. Carnahan¹⁷¹ S. Dildick¹⁷¹
 K. M. Ecklund¹⁷¹ P. J. Fernández Manteca¹⁷¹ S. Freed¹⁷¹ P. Gardner¹⁷¹ F. J. M. Geurts¹⁷¹ A. Kumar¹⁷¹ W. Li¹⁷¹
 B. P. Padley¹⁷¹ R. Redjimi¹⁷¹ J. Rotter¹⁷¹ S. Yang¹⁷¹ E. Yigitbasi¹⁷¹ Y. Zhang¹⁷¹ A. Bodek¹⁷²
 P. de Barbaro¹⁷² R. Demina¹⁷² J. L. Dulemba¹⁷² C. Fallon¹⁷² A. Garcia-Bellido¹⁷² O. Hindrichs¹⁷²
 A. Khukhunaishvili¹⁷² P. Parygin¹⁷² E. Popova¹⁷² R. Taus¹⁷² G. P. Van Onsem¹⁷² K. Goulianios¹⁷³
 B. Chiarito¹⁷⁴ J. P. Chou¹⁷⁴ Y. Gershtein¹⁷⁴ E. Halkiadakis¹⁷⁴ A. Hart¹⁷⁴ M. Heindl¹⁷⁴ D. Jaroslawski¹⁷⁴
 O. Karacheban^{174,y} I. Laflotte¹⁷⁴ A. Lath¹⁷⁴ R. Montalvo¹⁷⁴ K. Nash¹⁷⁴ M. Osherson¹⁷⁴ H. Routray¹⁷⁴
 S. Salur¹⁷⁴ S. Schnetzer¹⁷⁴ S. Somalwar¹⁷⁴ R. Stone¹⁷⁴ S. A. Thayil¹⁷⁴ S. Thomas¹⁷⁴ H. Wang¹⁷⁴ H. Acharya¹⁷⁵
 A. G. Delannoy¹⁷⁵ S. Fiorendi¹⁷⁵ T. Holmes¹⁷⁵ E. Nibigira¹⁷⁵ S. Spanier¹⁷⁵ O. Bouhali^{176,cq} M. Dalchenko¹⁷⁶
 A. Delgado¹⁷⁶ R. Eusebi¹⁷⁶ J. Gilmore¹⁷⁶ T. Huang¹⁷⁶ T. Kamon^{176,cr} H. Kim¹⁷⁶ S. Luo¹⁷⁶ S. Malhotra¹⁷⁶
 R. Mueller¹⁷⁶ D. Overton¹⁷⁶ D. Rathjens¹⁷⁶ A. Safonov¹⁷⁶ N. Akchurin¹⁷⁷ J. Damgov¹⁷⁷ V. Hegde¹⁷⁷
 K. Lamichhane¹⁷⁷ S. W. Lee¹⁷⁷ T. Mengke¹⁷⁷ S. Muthumuni¹⁷⁷ T. Peltola¹⁷⁷ I. Volobouev¹⁷⁷ A. Whitbeck¹⁷⁷
 E. Appelt¹⁷⁸ S. Greene¹⁷⁸ A. Gurrola¹⁷⁸ W. Johns¹⁷⁸ A. Melo¹⁷⁸ F. Romeo¹⁷⁸ P. Sheldon¹⁷⁸ S. Tuo¹⁷⁸
 J. Velkovska¹⁷⁸ J. Viinikainen¹⁷⁸ B. Cardwell¹⁷⁹ B. Cox¹⁷⁹ G. Cummings¹⁷⁹ J. Hakala¹⁷⁹ R. Hirosky¹⁷⁹
 A. Ledovskoy¹⁷⁹ A. Li¹⁷⁹ C. Neu¹⁷⁹ C. E. Perez Lara¹⁷⁹ P. E. Karchin¹⁸⁰ A. Aravind¹⁸¹ S. Banerjee¹⁸¹
 K. Black¹⁸¹ T. Bose¹⁸¹ S. Dasu¹⁸¹ I. De Bruyn¹⁸¹ P. Everaerts¹⁸¹ C. Galloni¹⁸¹ H. He¹⁸¹ M. Herndon¹⁸¹
 A. Herve¹⁸¹ C. K. Koraka¹⁸¹ A. Lanaro¹⁸¹ R. Loveless¹⁸¹ J. Madhusudanan Sreekala¹⁸¹ A. Mallampalli¹⁸¹
 A. Mohammadi¹⁸¹ S. Mondal¹⁸¹ G. Parida¹⁸¹ D. Pinna¹⁸¹ A. Savin¹⁸¹ V. Shang¹⁸¹ V. Sharma¹⁸¹ W. H. Smith¹⁸¹
 D. Teague¹⁸¹ H. F. Tsoi¹⁸¹ W. Vetens¹⁸¹ A. Warden¹⁸¹ S. Afanasiev¹⁸² V. Andreev¹⁸² Yu. Andreev¹⁸²
 T. Aushev¹⁸² M. Azarkin¹⁸² A. Babaev¹⁸² A. Belyaev¹⁸² V. Blinov^{182,cs} E. Boos¹⁸² V. Borshch¹⁸²
 D. Budkouski¹⁸² M. Chadeeva^{182,cs} V. Chekhovsky¹⁸² M. Danilov^{182,cs} A. Demiyanov¹⁸² A. Dermenev¹⁸²
 T. Dimova^{182,cs} I. Dremin¹⁸² V. Epshteyn¹⁸² A. Ershov¹⁸² G. Gavrilov¹⁸² V. Gavrilov¹⁸² S. Gninenko¹⁸²
 V. Golovtsov¹⁸² N. Golubev¹⁸² I. Golutvin¹⁸² I. Gorbunov¹⁸² A. Gribushin¹⁸² Y. Ivanov¹⁸² V. Kachanov¹⁸²
 L. Kardapoltsev^{182,cs} V. Karjavyne¹⁸² A. Karneyeu¹⁸² L. Khein¹⁸² V. Kim^{182,cs} M. Kirakosyan¹⁸²
 D. Kirpichnikov¹⁸² M. Kirsanov¹⁸² O. Kodolova^{182,ct} D. Konstantinov¹⁸² V. Korenkov¹⁸² V. Korotkikh¹⁸²
 A. Kozyrev^{182,cs} N. Krasnikov¹⁸² A. Lanev¹⁸² P. Levchenko¹⁸² A. Litomin¹⁸² N. Lychkovskaya¹⁸²
 V. Makarenko¹⁸² A. Malakhov¹⁸² V. Matveev^{182,cs,eu} V. Murzin¹⁸² A. Nikitenko^{182,ct,eu} S. Obraztsov¹⁸²

I. Ovtin^{182,cs}, V. Palichik¹⁸², V. Perelygin¹⁸², S. Petrushanko¹⁸², V. Popov¹⁸², O. Radchenko^{182,cs}, V. Rusinov¹⁸², M. Savina¹⁸², V. Savrin¹⁸², D. Selivanova¹⁸², V. Shalaev¹⁸², S. Shmatov¹⁸², S. Shulha¹⁸², Y. Skovpen^{182,cs}, S. Slabospitskii¹⁸², V. Smirnov¹⁸², A. Snigirev¹⁸², D. Sosnov¹⁸², V. Sulimov¹⁸², E. Tcherniaev¹⁸², A. Terkulov¹⁸², O. Teryaev¹⁸², I. Tlisova¹⁸², A. Toropin¹⁸², L. Uvarov¹⁸², A. Uzunian¹⁸², I. Vardanyan¹⁸², A. Vorobyev^{182,o}, N. Voytishin¹⁸², B. S. Yuldashev,^{182,cw} A. Zarubin¹⁸², I. Zhizhin¹⁸² and A. Zhokin¹⁸²

(CMS Collaboration)

¹*Yerevan Physics Institute, Yerevan, Armenia*

²*Institut für Hochenergiephysik, Vienna, Austria*

³*Universiteit Antwerpen, Antwerpen, Belgium*

⁴*Vrije Universiteit Brussel, Brussel, Belgium*

⁵*Université Libre de Bruxelles, Bruxelles, Belgium*

⁶*Ghent University, Ghent, Belgium*

⁷*Université Catholique de Louvain, Louvain-la-Neuve, Belgium*

⁸*Centro Brasileiro de Pesquisas Fisicas, Rio de Janeiro, Brazil*

⁹*Universidade do Estado do Rio de Janeiro, Rio de Janeiro, Brazil*

¹⁰*Universidade Estadual Paulista, Universidade Federal do ABC, São Paulo, Brazil*

¹¹*Institute for Nuclear Research and Nuclear Energy, Bulgarian Academy of Sciences, Sofia, Bulgaria*

¹²*University of Sofia, Sofia, Bulgaria*

¹³*Instituto De Alta Investigación, Universidad de Tarapacá, Casilla 7 D, Arica, Chile*

¹⁴*Beihang University, Beijing, China*

¹⁵*Department of Physics, Tsinghua University, Beijing, China*

¹⁶*Institute of High Energy Physics, Beijing, China*

¹⁷*State Key Laboratory of Nuclear Physics and Technology, Peking University, Beijing, China*

¹⁸*Sun Yat-Sen University, Guangzhou, China*

¹⁹*University of Science and Technology of China, Hefei, China*

²⁰*Institute of Modern Physics and Key Laboratory of Nuclear Physics and Ion-beam Application (MOE) - Fudan University, Shanghai, China*

²¹*Zhejiang University, Hangzhou, Zhejiang, China*

²²*Universidad de Los Andes, Bogota, Colombia*

²³*Universidad de Antioquia, Medellin, Colombia*

²⁴*University of Split, Faculty of Electrical Engineering, Mechanical Engineering and Naval Architecture, Split, Croatia*

²⁵*University of Split, Faculty of Science, Split, Croatia*

²⁶*Institute Rudjer Boskovic, Zagreb, Croatia*

²⁷*University of Cyprus, Nicosia, Cyprus*

²⁸*Charles University, Prague, Czech Republic*

²⁹*Escuela Politecnica Nacional, Quito, Ecuador*

³⁰*Universidad San Francisco de Quito, Quito, Ecuador*

³¹*Academy of Scientific Research and Technology of the Arab Republic of Egypt, Egyptian Network of High Energy Physics, Cairo, Egypt*

³²*Center for High Energy Physics (CHEP-FU), Fayoum University, El-Fayoum, Egypt*

³³*National Institute of Chemical Physics and Biophysics, Tallinn, Estonia*

³⁴*Department of Physics, University of Helsinki, Helsinki, Finland*

³⁵*Helsinki Institute of Physics, Helsinki, Finland*

³⁶*Lappeenranta-Lahti University of Technology, Lappeenranta, Finland*

³⁷*IRFU, CEA, Université Paris-Saclay, Gif-sur-Yvette, France*

³⁸*Laboratoire Leprince-Ringuet, CNRS/IN2P3, Ecole Polytechnique, Institut Polytechnique de Paris, Palaiseau, France*

³⁹*Université de Strasbourg, CNRS, IPHC UMR 7178, Strasbourg, France*

⁴⁰*Institut de Physique des 2 Infinis de Lyon (IP2I), Villeurbanne, France*

⁴¹*Georgian Technical University, Tbilisi, Georgia*

⁴²*RWTH Aachen University, I. Physikalisches Institut, Aachen, Germany*

⁴³*RWTH Aachen University, III. Physikalisches Institut A, Aachen, Germany*

⁴⁴*RWTH Aachen University, III. Physikalisches Institut B, Aachen, Germany*

⁴⁵*Deutsches Elektronen-Synchrotron, Hamburg, Germany*

⁴⁶*University of Hamburg, Hamburg, Germany*

⁴⁷*Karlsruhe Institut fuer Technologie, Karlsruhe, Germany*

⁴⁸*Institute of Nuclear and Particle Physics (INPP), NCSR Demokritos, Aghia Paraskevi, Greece*

⁴⁹*National and Kapodistrian University of Athens, Athens, Greece*

⁵⁰*National Technical University of Athens, Athens, Greece*

- ⁵¹*University of Ioánnina, Ioánnina, Greece*
⁵²*MTA-ELTE Lendület CMS Particle and Nuclear Physics Group, Eötvös Loránd University, Budapest, Hungary*
⁵³*Wigner Research Centre for Physics, Budapest, Hungary*
⁵⁴*Institute of Nuclear Research ATOMKI, Debrecen, Hungary*
⁵⁵*Institute of Physics, University of Debrecen, Debrecen, Hungary*
⁵⁶*Karoly Robert Campus, MATE Institute of Technology, Gyongyos, Hungary*
⁵⁷*Panjab University, Chandigarh, India*
⁵⁸*University of Delhi, Delhi, India*
⁵⁹*Saha Institute of Nuclear Physics, HBNI, Kolkata, India*
⁶⁰*Indian Institute of Technology Madras, Madras, India*
⁶¹*Bhabha Atomic Research Centre, Mumbai, India*
⁶²*Tata Institute of Fundamental Research-A, Mumbai, India*
⁶³*Tata Institute of Fundamental Research-B, Mumbai, India*
⁶⁴*National Institute of Science Education and Research, An OCC of Homi Bhabha National Institute, Bhubaneswar, Odisha, India*
⁶⁵*Indian Institute of Science Education and Research (IISER), Pune, India*
⁶⁶*Isfahan University of Technology, Isfahan, Iran*
⁶⁷*Institute for Research in Fundamental Sciences (IPM), Tehran, Iran*
⁶⁸*University College Dublin, Dublin, Ireland*
^{69a}*INFN Sezione di Bari, Bari, Italy*
^{69b}*Università di Bari, Bari, Italy*
^{69c}*Politecnico di Bari, Bari, Italy*
^{70a}*INFN Sezione di Bologna, Bologna, Italy*
^{70b}*Università di Bologna, Bologna, Italy*
^{71a}*INFN Sezione di Catania, Catania, Italy*
^{71b}*Università di Catania, Catania, Italy*
^{72a}*INFN Sezione di Firenze, Firenze, Italy*
^{72b}*Università di Firenze, Firenze, Italy*
⁷³*INFN Laboratori Nazionali di Frascati, Frascati, Italy*
^{74a}*INFN Sezione di Genova, Genova, Italy*
^{74b}*Università di Genova, Genova, Italy*
^{75a}*INFN Sezione di Milano-Bicocca, Milano, Italy*
^{75b}*Università di Milano-Bicocca, Milano, Italy*
^{76a}*INFN Sezione di Napoli, Napoli, Italy*
^{76b}*Università di Napoli 'Federico II', Napoli, Italy*
^{76c}*Università della Basilicata, Potenza, Italy*
^{76d}*Università G. Marconi, Roma, Italy*
^{77a}*INFN Sezione di Padova, Padova, Italy*
^{77b}*Università di Padova, Padova, Italy*
^{77c}*Università di Trento, Trento, Italy*
^{78a}*INFN Sezione di Pavia, Pavia, Italy*
^{78b}*Università di Pavia, Pavia, Italy*
^{79a}*INFN Sezione di Perugia, Perugia, Italy*
^{79b}*Università di Perugia, Perugia, Italy*
^{80a}*INFN Sezione di Pisa, Pisa, Italy*
^{80b}*Università di Pisa, Pisa, Italy*
^{80c}*Scuola Normale Superiore di Pisa, Pisa, Italy*
^{80d}*Università di Siena, Siena, Italy*
^{81a}*INFN Sezione di Roma, Roma, Italy*
^{81b}*Sapienza Università di Roma, Roma, Italy*
^{82a}*INFN Sezione di Torino, Torino, Italy*
^{82b}*Università di Torino, Torino, Italy*
^{82c}*Università del Piemonte Orientale, Novara, Italy*
^{83a}*INFN Sezione di Trieste, Trieste, Italy*
^{83b}*Università di Trieste, Trieste, Italy*
⁸⁴*Kyungpook National University, Daegu, Korea*
⁸⁵*Chonnam National University, Institute for Universe and Elementary Particles, Kwangju, Korea*
⁸⁶*Hanyang University, Seoul, Korea*
⁸⁷*Korea University, Seoul, Korea*
⁸⁸*Kyung Hee University, Department of Physics, Seoul, Korea*

- ⁸⁹Sejong University, Seoul, Korea
⁹⁰Seoul National University, Seoul, Korea
⁹¹University of Seoul, Seoul, Korea
⁹²Yonsei University, Department of Physics, Seoul, Korea
⁹³Sungkyunkwan University, Suwon, Korea
⁹⁴College of Engineering and Technology, American University of the Middle East (AUM), Dasman, Kuwait
⁹⁵Riga Technical University, Riga, Latvia
⁹⁶Vilnius University, Vilnius, Lithuania
⁹⁷National Centre for Particle Physics, Universiti Malaya, Kuala Lumpur, Malaysia
⁹⁸Universidad de Sonora (UNISON), Hermosillo, Mexico
⁹⁹Centro de Investigacion y de Estudios Avanzados del IPN, Mexico City, Mexico
¹⁰⁰Universidad Iberoamericana, Mexico City, Mexico
¹⁰¹Benemerita Universidad Autonoma de Puebla, Puebla, Mexico
¹⁰²University of Montenegro, Podgorica, Montenegro
¹⁰³National Centre for Physics, Quaid-I-Azam University, Islamabad, Pakistan
¹⁰⁴AGH University of Science and Technology Faculty of Computer Science, Electronics and Telecommunications, Krakow, Poland
¹⁰⁵National Centre for Nuclear Research, Swierk, Poland
¹⁰⁶Institute of Experimental Physics, Faculty of Physics, University of Warsaw, Warsaw, Poland
¹⁰⁷Laboratório de Instrumentação e Física Experimental de Partículas, Lisboa, Portugal
¹⁰⁸VINCA Institute of Nuclear Sciences, University of Belgrade, Belgrade, Serbia
¹⁰⁹Centro de Investigaciones Energéticas Medioambientales y Tecnológicas (CIEMAT), Madrid, Spain
¹¹⁰Universidad Autónoma de Madrid, Madrid, Spain
¹¹¹Universidad de Oviedo, Instituto Universitario de Ciencias y Tecnologías Espaciales de Asturias (ICTEA), Oviedo, Spain
¹¹²Instituto de Física de Cantabria (IFCA), CSIC-Universidad de Cantabria, Santander, Spain
¹¹³University of Colombo, Colombo, Sri Lanka
¹¹⁴University of Ruhuna, Department of Physics, Matara, Sri Lanka
¹¹⁵CERN, European Organization for Nuclear Research, Geneva, Switzerland
¹¹⁶Paul Scherrer Institut, Villigen, Switzerland
¹¹⁷ETH Zurich - Institute for Particle Physics and Astrophysics (IPA), Zurich, Switzerland
¹¹⁸Universität Zürich, Zurich, Switzerland
¹¹⁹National Central University, Chung-Li, Taiwan
¹²⁰National Taiwan University (NTU), Taipei, Taiwan
¹²¹Chulalongkorn University, Faculty of Science, Department of Physics, Bangkok, Thailand
¹²²Çukurova University, Physics Department, Science and Art Faculty, Adana, Turkey
¹²³Middle East Technical University, Physics Department, Ankara, Turkey
¹²⁴Bogazici University, Istanbul, Turkey
¹²⁵Istanbul Technical University, Istanbul, Turkey
¹²⁶Istanbul University, Istanbul, Turkey
¹²⁷Institute for Scintillation Materials of National Academy of Science of Ukraine, Kharkiv, Ukraine
¹²⁸National Science Centre, Kharkiv Institute of Physics and Technology, Kharkiv, Ukraine
¹²⁹University of Bristol, Bristol, United Kingdom
¹³⁰Rutherford Appleton Laboratory, Didcot, United Kingdom
¹³¹Imperial College, London, United Kingdom
¹³²Brunel University, Uxbridge, United Kingdom
¹³³Baylor University, Waco, Texas, USA
¹³⁴Catholic University of America, Washington, DC, USA
¹³⁵The University of Alabama, Tuscaloosa, Alabama, USA
¹³⁶Boston University, Boston, Massachusetts, USA
¹³⁷Brown University, Providence, Rhode Island, USA
¹³⁸University of California, Davis, Davis, California, USA
¹³⁹University of California, Los Angeles, California, USA
¹⁴⁰University of California, Riverside, Riverside, California, USA
¹⁴¹University of California, San Diego, La Jolla, California, USA
¹⁴²University of California, Santa Barbara - Department of Physics, Santa Barbara, California, USA
¹⁴³California Institute of Technology, Pasadena, California, USA
¹⁴⁴Carnegie Mellon University, Pittsburgh, Pennsylvania, USA
¹⁴⁵University of Colorado Boulder, Boulder, Colorado, USA
¹⁴⁶Cornell University, Ithaca, New York, USA
¹⁴⁷Fermi National Accelerator Laboratory, Batavia, Illinois, USA

- ¹⁴⁸*University of Florida, Gainesville, Florida, USA*
¹⁴⁹*Florida State University, Tallahassee, Florida, USA*
¹⁵⁰*Florida Institute of Technology, Melbourne, Florida, USA*
¹⁵¹*University of Illinois at Chicago (UIC), Chicago, Illinois, USA*
¹⁵²*The University of Iowa, Iowa City, Iowa, USA*
¹⁵³*Johns Hopkins University, Baltimore, Maryland, USA*
¹⁵⁴*The University of Kansas, Lawrence, Kansas, USA*
¹⁵⁵*Kansas State University, Manhattan, Kansas, USA*
¹⁵⁶*Lawrence Livermore National Laboratory, Livermore, California, USA*
¹⁵⁷*University of Maryland, College Park, Maryland, USA*
¹⁵⁸*Massachusetts Institute of Technology, Cambridge, Massachusetts, USA*
¹⁵⁹*University of Minnesota, Minneapolis, Minnesota, USA*
¹⁶⁰*University of Mississippi, Oxford, Mississippi, USA*
¹⁶¹*University of Nebraska-Lincoln, Lincoln, Nebraska, USA*
¹⁶²*State University of New York at Buffalo, Buffalo, New York, USA*
¹⁶³*Northeastern University, Boston, Massachusetts, USA*
¹⁶⁴*Northwestern University, Evanston, Illinois, USA*
¹⁶⁵*University of Notre Dame, Notre Dame, Indiana, USA*
¹⁶⁶*The Ohio State University, Columbus, Ohio, USA*
¹⁶⁷*Princeton University, Princeton, New Jersey, USA*
¹⁶⁸*University of Puerto Rico, Mayaguez, Puerto Rico, USA*
¹⁶⁹*Purdue University, West Lafayette, Indiana, USA*
¹⁷⁰*Purdue University Northwest, Hammond, Indiana, USA*
¹⁷¹*Rice University, Houston, Texas, USA*
¹⁷²*University of Rochester, Rochester, New York, USA*
¹⁷³*The Rockefeller University, New York, New York, USA*
¹⁷⁴*Rutgers, The State University of New Jersey, Piscataway, New Jersey, USA*
¹⁷⁵*University of Tennessee, Knoxville, Tennessee, USA*
¹⁷⁶*Texas A&M University, College Station, Texas, USA*
¹⁷⁷*Texas Tech University, Lubbock, Texas, USA*
¹⁷⁸*Vanderbilt University, Nashville, Tennessee, USA*
¹⁷⁹*University of Virginia, Charlottesville, Virginia, USA*
¹⁸⁰*Wayne State University, Detroit, Michigan, USA*
¹⁸¹*University of Wisconsin - Madison, Madison, Wisconsin, USA*

¹⁸²*Authors affiliated with an institute or an international laboratory covered by a cooperation agreement with CERN.*

^aAlso at Yerevan State University, Yerevan, Armenia.

^bAlso at TU Wien, Vienna, Austria.

^cAlso at Institute of Basic and Applied Sciences, Faculty of Engineering, Arab Academy for Science, Technology and Maritime Transport, Alexandria, Egypt.

^dAlso at Université Libre de Bruxelles, Bruxelles, Belgium.

^eAlso at Universidade Estadual de Campinas, Campinas, Brazil.

^fAlso at Federal University of Rio Grande do Sul, Porto Alegre, Brazil.

^gAlso at UFMS, Nova Andradina, Brazil.

^hAlso at University of Chinese Academy of Sciences, Beijing, China.

ⁱAlso at Nanjing Normal University, Nanjing, China.

^jNow at The University of Iowa, Iowa City, Iowa, USA.

^kAlso at an institute or an international laboratory covered by a cooperation agreement with CERN.

^lAlso at Cairo University, Cairo, Egypt.

^mAlso at Suez University, Suez, Egypt.

ⁿNow at British University in Egypt, Cairo, Egypt.

^oDeceased.

^pAlso at Purdue University, West Lafayette, Indiana, USA.

^qAlso at Université de Haute Alsace, Mulhouse, France.

^rAlso at Department of Physics, Tsinghua University, Beijing, China.

^sAlso at The University of the State of Amazonas, Manaus, Brazil.

^tAlso at Erzincan Binali Yildirim University, Erzincan, Turkey.

^uAlso at University of Hamburg, Hamburg, Germany.

^vAlso at RWTH Aachen University, III. Physikalisches Institut A, Aachen, Germany.

^wAlso at Isfahan University of Technology, Isfahan, Iran.

^xAlso at Bergische University Wuppertal (BUW), Wuppertal, Germany.

^yAlso at Brandenburg University of Technology, Cottbus, Germany.

^zAlso at Forschungszentrum Jülich, Juelich, Germany.

^{aa}Also at CERN, European Organization for Nuclear Research, Geneva, Switzerland.

^{ab}Also at Physics Department, Faculty of Science, Assiut University, Assiut, Egypt.

^{ac}Also at Wigner Research Centre for Physics, Budapest, Hungary.

^{ad}Also at Institute of Physics, University of Debrecen, Debrecen, Hungary.

^{ae}Also at Institute of Nuclear Research ATOMKI, Debrecen, Hungary.

^{af}Now at Universitatea Babes-Bolyai - Facultatea de Fizica, Cluj-Napoca, Romania.

^{ag}Also at Faculty of Informatics, University of Debrecen, Debrecen, Hungary.

^{ah}Also at Punjab Agricultural University, Ludhiana, India.

^{ai}Also at UPES - University of Petroleum and Energy Studies, Dehradun, India.

^{aj}Also at University of Visva-Bharati, Santiniketan, India.

^{ak}Also at University of Hyderabad, Hyderabad, India.

^{al}Also at Indian Institute of Science (IISc), Bangalore, India.

^{am}Also at Indian Institute of Technology (IIT), Mumbai, India.

^{an}Also at IIT Bhubaneswar, Bhubaneswar, India.

^{ao}Also at Institute of Physics, Bhubaneswar, India.

^{ap}Also at Deutsches Elektronen-Synchrotron, Hamburg, Germany.

^{aq}Now at Department of Physics, Isfahan University of Technology, Isfahan, Iran.

^{ar}Also at Sharif University of Technology, Tehran, Iran.

^{as}Also at Department of Physics, University of Science and Technology of Mazandaran, Behshahr, Iran.

^{at}Also at Helwan University, Cairo, Egypt.

^{au}Also at Italian National Agency for New Technologies, Energy and Sustainable Economic Development, Bologna, Italy.

^{av}Also at Centro Siciliano di Fisica Nucleare e di Struttura Della Materia, Catania, Italy.

^{aw}Also at Università degli Studi Guglielmo Marconi, Roma, Italy.

^{ax}Also at Scuola Superiore Meridionale, Università di Napoli 'Federico II', Napoli, Italy.

^{ay}Also at Fermi National Accelerator Laboratory, Batavia, Illinois, USA.

^{az}Also at Università di Napoli 'Federico II', Napoli, Italy.

^{ba}Also at Ain Shams University, Cairo, Egypt.

^{bb}Also at Consiglio Nazionale delle Ricerche - Istituto Officina dei Materiali, Perugia, Italy.

^{bc}Also at Riga Technical University, Riga, Latvia.

^{bd}Also at Department of Applied Physics, Faculty of Science and Technology, Universiti Kebangsaan Malaysia, Bangi, Malaysia.

^{be}Also at Consejo Nacional de Ciencia y Tecnología, Mexico City, Mexico.

^{bf}Also at IRFU, CEA, Université Paris-Saclay, Gif-sur-Yvette, France.

^{bg}Also at Faculty of Physics, University of Belgrade, Belgrade, Serbia.

^{bh}Also at Trincomalee Campus, Eastern University, Sri Lanka, Nilaveli, Sri Lanka.

^{bi}Also at INFN Sezione di Pavia, Università di Pavia, Pavia, Italy.

^{bj}Also at National and Kapodistrian University of Athens, Athens, Greece.

^{bk}Also at Ecole Polytechnique Fédérale Lausanne, Lausanne, Switzerland.

^{bl}Also at Universität Zürich, Zurich, Switzerland.

^{bm}Also at Stefan Meyer Institute for Subatomic Physics, Vienna, Austria.

^{bn}Also at Laboratoire d'Annecy-le-Vieux de Physique des Particules, IN2P3-CNRS, Annecy-le-Vieux, France.

^{bo}Also at Near East University, Research Center of Experimental Health Science, Mersin, Turkey.

^{bp}Also at Konya Technical University, Konya, Turkey.

^{rq}Also at Izmir Bakircay University, Izmir, Turkey.

^{pr}Also at Adiyaman University, Adiyaman, Turkey.

^{ps}Also at Istanbul Gedik University, Istanbul, Turkey.

^{pt}Also at Necmettin Erbakan University, Konya, Turkey.

^{pu}Also at Bozok Universitetesi Rektörlüğü, Yozgat, Turkey.

^{pv}Also at Marmara University, Istanbul, Turkey.

^{pw}Also at Milli Savunma University, Istanbul, Turkey.

^{qx}Also at Kafkas University, Kars, Turkey.

^{by}Also at Hacettepe University, Ankara, Turkey.

^{bz}Also at Istanbul University - Cerrahpasa, Faculty of Engineering, Istanbul, Turkey.

^{ca}Also at Ozyegin University, Istanbul, Turkey.

^{cb}Also at Vrije Universiteit Brussel, Brussel, Belgium.

^{cc}Also at School of Physics and Astronomy, University of Southampton, Southampton, United Kingdom.

^{cd}Also at University of Bristol, Bristol, United Kingdom.

^{ce}Also at IPPP Durham University, Durham, United Kingdom.

^{cf}Also at Monash University, Faculty of Science, Clayton, Australia.

^{cg}Also at Università di Torino, Torino, Italy.

^{ch}Also at Bethel University, St. Paul, Minnesota, USA.

^{ci}Also at Karamanoğlu Mehmetbey University, Karaman, Turkey.

^{cj}Also at California Institute of Technology, Pasadena, California, USA.

^{ck}Also at United States Naval Academy, Annapolis, Maryland, USA.

^{cl}Also at University of Florida, Gainesville, Florida, USA.

^{cm}Also at Bingol University, Bingol, Turkey.

^{cn}Also at Georgian Technical University, Tbilisi, Georgia.

^{co}Also at Sinop University, Sinop, Turkey.

^{cp}Also at Erciyes University, Kayseri, Turkey.

^{cq}Also at Texas A&M University at Qatar, Doha, Qatar.

^{cr}Also at Kyungpook National University, Daegu, Korea.

^{cs}Also at another institute or international laboratory covered by a cooperation agreement with CERN.

^{ct}Also at Yerevan Physics Institute, Yerevan, Armenia.

^{cu}Now at another institute or international laboratory covered by a cooperation agreement with CERN.

^{cv}Also at Imperial College, London, United Kingdom.

^{cw}Also at Institute of Nuclear Physics of the Uzbekistan Academy of Sciences, Tashkent, Uzbekistan.